Synoptic Circulation and Land Surface Influences on Convection in the Midwest U.S. "Corn Belt" during the Summers of 1999 and 2000. Part I: Composite Synoptic Environments

ANDREW M. CARLETON

Department of Geography, and Earth and Environmental Systems Institute, The Pennsylvania State University, University Park, Pennsylvania

DAVID L. ARNOLD

Department of Geography, Frostburg State University, Frostburg, Maryland

DAVID J. TRAVIS

Department of Geography and Geology, University of Wisconsin—Whitewater, Whitewater, Wisconsin

STEVE CURRAN

Department of Geography, The Pennsylvania State University, University Park, Pennsylvania

JIMMY O. ADEGOKE

Department of Geosciences, University of Missouri, Kansas City, Missouri

(Manuscript received 10 July 2006, in final form 5 November 2007)

ABSTRACT

In the Midwest U.S. Corn Belt, the 1999 and 2000 summer seasons (15 June–15 September) expressed contrasting spatial patterns and magnitudes of precipitation (1999: dry; 2000: normal to moist). Distinct from the numerical modeling approach often used in studies of land surface–climate interactions, a "synoptic climatological" (i.e., stratified composite) approach is applied to observation data (e.g., precipitation, radar, and atmospheric reanalyses) to determine the relative influences of "top-down" synoptic atmospheric circulation (Part I, this paper) and "bottom-up" land surface mesoscale conditions (Part II) on the predominantly convective precipitation variations. Because mesoscale modeling suggests that the free-atmosphere wind speed ("background wind") regulates the land surface–atmosphere mesoscale interaction, each day's spatial range of wind speed at 500 hPa [**V**(500)] over the Central Corn Belt (CCB) is classified into one of five categories ranging from "weak flow" to "jet maximum." Deep convective activity (i.e., presence/absence and morphological signature type) is determined for each afternoon and early evening period from the Next Generation Weather Radar (NEXRAD) imagery. Frequencies of the resulting background wind–convection joint occurrence types for the 1999 and 2000 summer seasons are examined in the context of the statistics determined for summers in the longer period of 1996–2001, and also compose categories for which NCEP–NCAR reanalysis (NNR) fields are averaged to yield synoptic composite environments for the two study seasons. The latter composites are compared visually with high-resolution (spatial) composites of precipitation to help identify the influence of top-down climate controls.

The analysis confirms that reduced (increased) organization of radar-indicated deep convection tends to occur with weaker (stronger) background flow. The summers of 1999 and 2000 differ from one another in terms of background flow and convective activity, but more so with respect to the six-summer averages, indicating that a fuller explanation of the precipitation differences in the two summers must be sought in the analysis of additional synoptic meteorological variables. The composite synoptic conditions on convection (CV) days (no convection (NC) days) in 1999 and 2000 are generalized as follows: low pressure incoming

Corresponding author address: Andrew M. Carleton, Department of Geography, and Earth and Environmental Systems Institute (EESI), The Pennsylvania State University, University Park, PA 16802.
E-mail: carleton@essc.psu.edu

DOI: 10.1175/2007JCLI1578.1

© 2008 American Meteorological Society

from the west (high pressure or ridging), southerly (northerly) lower-tropospheric winds, positive (negative) anomalies of moisture in the lower troposphere, rising (sinking) air in the midtroposphere, and a location south of the upper-tropospheric jet maximum (absence of an upper-tropospheric jet or one located just south of the area). Features resembling the "northerly low-level jets" identified in previous studies for the Great Plains are present on some NC-day composites. On CV days the spatial synchronization of synoptic features implying baroclinity increases with increasing background wind speed. The CV and NC composites differ least on days of weaker flow, and there are small areas within the CCB having no obvious association between precipitation elevated amounts and synoptic circulation features favoring the upward motion of air. These spatial incongruities imply a contributory influence of "stationary" (i.e., climatic) land surface mesoscale processes in convective activity, which are examined in Part II.

1. Introduction

a. Context

The humid lowlands of the Midwestern U.S. "Corn Belt" ("CB") encompass the southern and western Great Lakes region (e.g., Sharratt et al. 2001), and compose large parts of the following states: Illinois, Indiana, Wisconsin, Ohio, Iowa, Missouri, and Michigan (Fig. 1). The CB is important for domestic primary production and the global economy (e.g., Hayes and Decker 1996): agriculture dominantly is rain fed, and consists mostly of maize (i.e., corn), with the secondary production being soybeans (e.g., Heim et al. 2003, their Figs. 2 and 3; Hicke and Lobell 2004; Westcott et al. 2005). Accordingly, warm-season climate variations significantly impact agriculture in the CB (Shafer and Mjedle 1994; Phillips et al. 1999; Changnon and Winstanley 2000; Hu and Buyanovsky 2003). Over the past two decades, climate variations there have ranged from extreme drought (1988) to extreme wetness (1993; see Namias 1991; Mo et al. 1991; Betts et al. 1996; Trenberth and Guillemot 1996; Oglesby et al. 2001). Although deleterious in their impacts on agriculture, such extreme regional-scale climate anomalies, by definition, occur less frequently than the spatially less extensive and lower-magnitude interannual variations, which still influence crop yields (Changnon 2004). However, relatively little attention has been paid to understanding the climate dynamics of these "typical" (i.e., more frequently occurring) departures of warm-season precipitation from longer-term normals in the Midwest (cf. Changnon and Hollinger 2003).

Teleconnections linking sea–air interactions in the tropical and subtropical Pacific Ocean (notably ENSO) have been implicated in U.S.-wide climate variations (e.g., Markowski and North 2003; Quan et al. 2006), including those in the central United States (Montroy et al. 1998; Englehart and Douglas 2002; Wannebo and Rosenzweig 2003). However, both modeling and observational studies suggest that remote forcing alone is insufficient to maintain climate anomalies of a particular sign through the growing season in interior continental locations: local–regional-scale interactions between the atmosphere and land surface variables (vegetation, "surface wetness" and soil moisture, topography) appear important (Koster and Suarez 1995, 2004; Pan et al. 1995; Giorgi et al. 1996; Xue et al. 1996; Fennessy and Shukla 1999; Pielke et al. 1999; Pal and Eltahir 2001; Tsvetsinskaya et al. 2001; Hong and Kalnay 2002; Dirmeyer 2003; Dirmeyer et al. 2003; Sud et al. 2003; Zangvil et al. 2004). For example, the predictability of warm-season surface temperatures for the central United States is improved when the previous month's precipitation or soil moisture is considered (Huang and Van den Dool 1993; Durre et al. 2000; Mo 2003; Van den Dool et al. 2003; Alfaro et al. 2006). Such improved predictability may also extend to summertime precipitation in the central United States (Douville 2003; Koster et al. 2003, 2004; Yang et al. 2004; Kanae et al. 2006).

The warm-season precipitation maximum in the Midwest CB, like that of the Great Plains located farther west, results primarily from convective activity (e.g., Richman and Lamb 1985; Winkler et al. 1988; Changnon 2001). Although deep convection inherently is a mesoscale phenomenon, it takes place within synoptic-scale atmospheric environments that permit upward motion of air through a considerable depth (e.g., Portis and Lamb 1988; Birmingham and Lamb 1994; Doran and Zhong 2000). When convection occurs in environments lacking significant synoptically forced ascent, a land surface influence often is inferred (e.g., Haragan 1978; Schaaf et al. 1988). In the central United States, convective precipitation and its interannual variations result from moisture both advected from the Gulf of Mexico (e.g., Roads et al. 1994; Seneviratne et al. 2004) and derived locally, or "recycled," from land surface evaporation (Burde et al. 1996; Bosilovich and Schubert 2001; Brubaker et al. 2001; Hu and Feng 2001; Zangvil et al. 2001, 2004; Ruiz-Barradas and Nigam 2005). Precipitation fluctuations dominate daily and subdaily time scales (Joseph et al. 2000), and comprise showers and thunderstorms often organized into mesoscale convective systems (MCSs) and quasi-linear

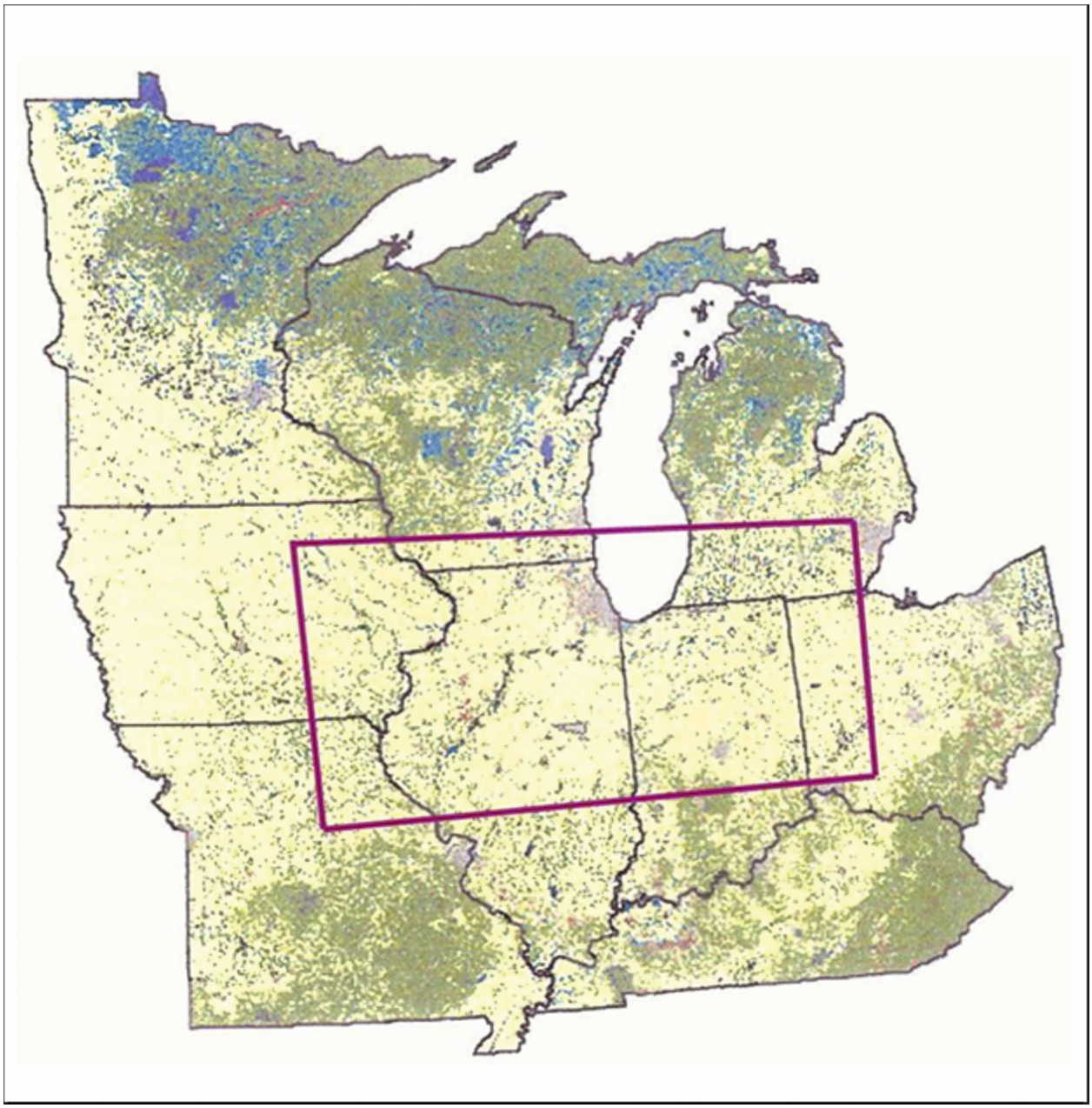

FIG. 1. Primary LULC types for the Midwest U.S. CB and adjacent areas, designated as follows: agriculture (yellow), forest (green), urban (gray), rangeland (rust), water (dark blue), wetland (light blue), and barren land (red). The magenta quadrilateral encloses the CCB, comprising mostly agricultural land. (Source: USGS online data archive.)

convective systems (QLCSs) by the larger-scale upper-tropospheric dynamics (e.g., differential positive vorticity advection, divergence), or along fronts (Zipser 1982; Hane 1986; Parker and Johnson 2000; Trapp et al. 2005). The dynamical processes are associated with jet stream maxima, short waves, surface cyclones, and warm fronts (Maddox 1983; Weisman and Klemp 1984; Fritsch et al. 1986; Moller et al. 1994; Schubert et al. 1998; Carbone et al. 2002; Ashley et al. 2003). At other times, deep convection is unorganized spatially and shows a closer association with the diurnal cycle of solar heating at the earth's surface (Tian et al. 2005). Accordingly, scattered or isolated deep convection is likely when the larger-scale atmospheric forcing is weak through relaxed height and temperature gradients (i.e., reduced baroclinity), which reduces vertical wind shear (O'Neal 1996; Carleton et al. 2001; Hanesiak et al. 2004). Atmospheric transient discontinuities, such as

the outflow boundaries derived from recent showers and thunderstorms, can generate or reignite convection, particularly where they intersect (e.g., Purdom 1976; Maddox et al. 1980; Wilson and Schreiber 1986; Crook 1996).

Surface–atmosphere interactions are important for convective cloud and precipitation development (Betts 2004) when the free atmosphere is coupled with the planetary boundary layer (PBL; Weaver and Avissar 2001; Segal et al. 2002). Thus, land surface conditions of soil moisture and vegetation, including those related to land use and land cover (LULC), influence deep convection (Carleton et al. 1994, 2001; Chen and Avissar 1994a; Brown and Arnold 1998; Pielke 2001; Weaver and Avissar 2001; Cheng and Cotton 2004) given "favorable" ambient humidity (e.g., Pielke and Zeng 1989; Rabin et al. 1990; Rabin and Martin 1996; Findell and Eltahir 2003a,b) and associated synoptic–dynamic conditions (Weaver 2004a,b). Averaged over the long term, land surface variables tend to be interrelated at a given location (e.g., Teuling and Troch 2005). Published modeling studies of land surface–atmosphere interactions are more numerous than those that are observationally based, and most of the latter have been conducted for drier regions than the Midwest; notably, the Great Plains (e.g., Santanello et al. 2005). These studies suggest that the land surface contribution to deep convection is most apparent when a lack of mixing in the PBL permits expression of the spatial contrasts in soil moisture and/or LULC type; for example, under "weak flow" conditions in the free atmosphere (Segal et al. 1989; Rabin et al. 1990; Klink 1995; Wetzel et al. 1996; Wang et al. 2000; Hanesiak et al. 2004). Then, weakly sheared moist convection (Wetzel 1990) results from enhanced convergence of low-level moisture, possibly associated with nonclassical (i.e., non–sea breeze) mesoscale circulations (NCMCs) that develop between adjacent contrasting land surface types (Mahfouf et al. 1987; Segal et al. 1988; Segal and Arritt 1992; Dalu et al. 2000). There are hints of the importance of land surface boundaries in convective initiation even in strongly sheared environments (e.g., Doswell 1987; Wilson et al. 1992; Hane et al. 2002; Weaver and Avissar 2001; Weaver 2004a), although the role of NCMCs continues to be debated (cf. Doran and Zhong 2002; Weaver and Avissar 2002).

b. The Midwest Central Corn Belt (CCB) study region

The greater attention paid to convective activity, and its associated physical mechanisms such as NCMCs, in the Great Plains versus the Midwest CB (e.g., Barnston and Schickedanz 1984; McCorcle 1988; Pielke and Zeng 1989; Rabin et al. 1990; Shaw and Doran 2001; Weaver and Avissar 2001; Weaver 2004a,b; McPherson et al. 2004) makes it tempting to assume that convective environments are directly transferable between the two regions. However, there are important climatological differences necessitating separate study of the Midwest for synoptic atmospheric and land surface influences on convection (Fig. 1). In the Midwest (Great Plains), precipitation mean amounts are the greater (lesser) and potential evapotranspiration values are lower (higher). Also, higher mean values of boundary layer humidity—denoted by the average surface dewpoint temperature—occur earlier in the warm season in the Great Plains contrasted with the Midwest (Gaffen and Ross 1999). The Midwest represents a transition zone from thunderstorm precipitation that is dominantly nocturnal to the west, and frequently associated with MCSs, to one that peaks in the afternoon and early evening hours located to the east (Easterling 1989; Higgins et al. 1997, their Figs. 3 and 4; Zajac and Rutledge 2001, their Fig. 10b; Orville and Huffines 2001, their Fig. 21).

The Midwest also comprises a distinct region in terms of the synoptic atmospheric conditions promoting summertime convective activity, and the likely role of land surface–atmosphere interactions: it is less influenced by southerly low-level jets (LLJs) than the Great Plains (cf. Pitchford and London 1962; Schubert et al. 1998; Banta et al. 2002; Zaitao et al. 2004), and the lack of orography over wide areas within the Central Corn Belt (CCB; Fig. 1) means that the topography is dominated by boundaries between major LULC types, especially croplands and remnant forest (Rabin and Martin 1996; Travis 1997). These boundaries are the result of substantial land-cover alterations by humans over the past 150 yr (agriculture, removal of ecotones), and have impacted near-surface climate (Copeland et al. 1996; Bonan 2001; Baidya Roy et al. 2003). Arguably, these land-cover changes have been more dramatic than those in the Great Plains, except for areas converted from pasture to irrigated agriculture (Pielke and Zeng 1989; Chase et al. 1999; Moore and Rojstaczer 2001; Adegoke et al. 2003, 2007). The Midwest is an integral part of the Mississippi River basin (e.g., Twine et al. 2004), the study of which is a continuing focus of the Global Energy and Water Cycle Experiment (GEWEX) Continental-Scale International Project (GCIP; Coughlan and Avissar 1996; Oglesby et al. 2001; Maurer and Lettenmaier 2003; Roads et al. 2003; Sudradjat et al. 2003).

It is apparent that the CCB (Fig. 1) represents a close-to-ideal region to determine from observation

data, as distinct from numerical modeling, the relative contributions of "top-down" synoptic atmospheric and "bottom-up" mesoscale land surface conditions to summertime deep convection. An informative approach is to compare synoptic atmospheric circulation and land surface conditions for two warm seasons that are dissimilar yet broadly representative of the climate variations typically experienced (Liu et al. 2004; Zangvil et al. 2004). We undertake such an empirical analysis for the "consecutive" summer seasons (15 June–15 September) of 1999 and 2000, respectively, dry and normal to moist in the CCB. Moreover, we situate synoptically these 2 yr within the six-summer period 1996–2001. Summer 2000 is particularly appropriate for study because the National Oceanic and Atmospheric Administration (NOAA) seasonal climate forecast, issued in spring 2000, projected an intensification of the dry conditions from summer 1999 (Changnon 2002, 2004), and a substantial number of farmers modified their crop planting schedules in light of this forecast. In this paper (Part I), we derive a stratified composite analysis from daily averaged atmospheric reanalyses to yield the synoptic circulation features associated with deep convection—and its absence—in the CCB for the two summers. We intercompare composite maps of the synoptic conditions and precipitation recorded at high spatial resolutions, to identify the influence of the synoptic circulation from the spatial coincidence or near coincidence of precipitation maxima and those features accompanying and denoting widespread upward motion of air. In Carleton et al. (2008, hereafter Part II) we determine the coinfluence of land surface conditions, specifically LULC boundaries, on the 1999 and 2000 summer composite precipitation maxima in the CCB for representative background flow categories and subareas lacking an obvious association with strongly rising air in the free atmosphere.

2. Overview of the contrasting summers, 1999 and 2000

Summer-season totals of precipitation for 1999 and 2000 (Fig. 2) are derived using the "Surface Land Daily Cooperative Summary of the Day" (DSI-3200) dataset for the United States (NCDC 2003), described more fully in section 4b. In the summer of 1999 (Fig. 2a), the CCB (Fig. 1) experienced generally low precipitation amounts while high totals occurred through much of the northern ("Upper") Midwest. By contrast, summer 2000 precipitation amounts (Fig. 2b) were higher in the CCB and extending to the southward, across southern Illinois and Indiana. A significant contribution to the latter high values came from convective systems that developed in eastern Missouri and southwest Illinois, and propagated eastward, in the first 2–3 weeks of August (Adegoke et al. 2006; Tuttle and Davis 2006). The possible contributory influence of the land surface on these high precipitation totals is examined in Part II [section 4b(4)].

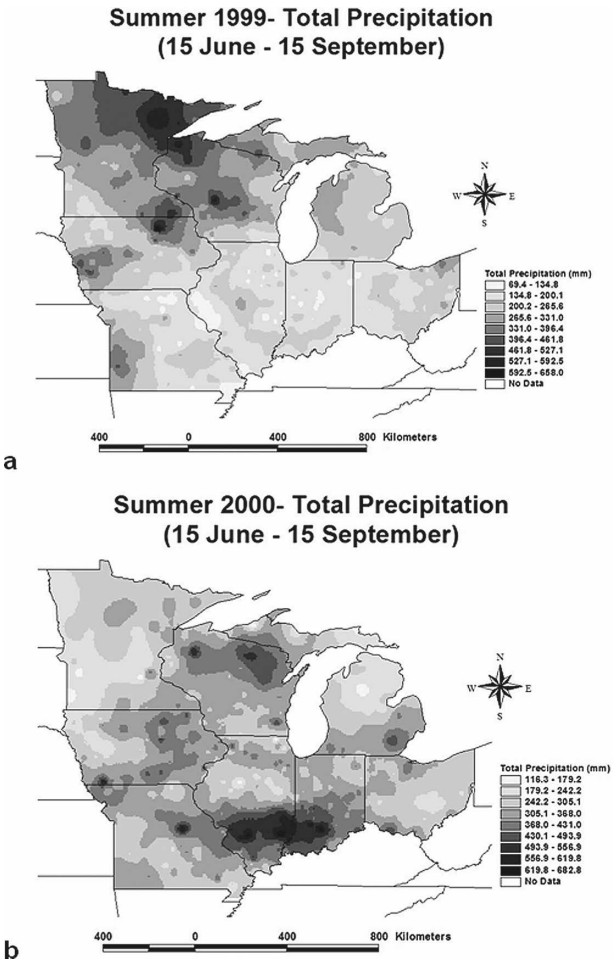

FIG. 2. Summer-season (15 Jun–15 Sep) total precipitation (mm) for the Midwest region: (a) 1999 and (b) 2000.

The between-summer differences in surface-recorded precipitation (Fig. 2) for both the CCB and larger Midwest region, correspond to large differences in the mean (15 June–15 September) circulation climates for 1999 and 2000: maps of summer-season atmospheric average anomalies (Fig. 3), utilizing the National Centers for Environmental Prediction–National Center for Atmospheric Research (NCEP–NCAR) reanalyses (NNR; section 4a), confirm a strong synoptic influence on precipitation when atmospheric data are averaged temporally. For example, anomaly patterns of the outgoing longwave radiation (OLR; Figs. 3a,b) show posi-

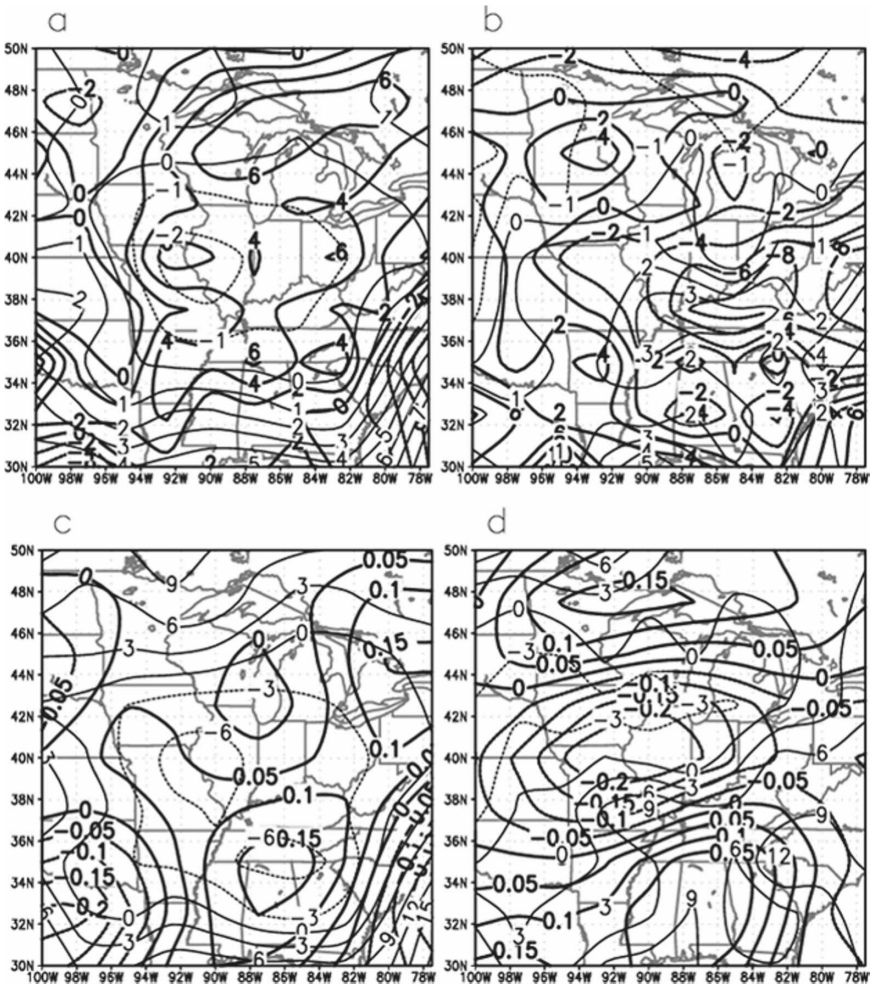

FIG. 3. Summer-season averaged (15 Jun–15 Sep) anomaly maps of selected NNR climate variables, as follows: OLR (W m^{-2}; darker lines) and PW (kg m^{-2}) for (a) 1999 and (b) 2000; omega (hPa s^{-1}) at 700 hPa [ω(700), darker lines] and RH at 700 hPa [RH(700), %] for (c) 1999 and (d) 2000; geopotential height (m) at 500 hPa [Z(500), darker lines] and zonal wind (m s^{-1}) at 500 hPa [u(500)] for (e) 1999 and (f) 2000; meridional component of the wind (m s^{-1}) at 700 hPa [υ(700), darker lines] and SLP (hPa) for (g) 1999 and (h) 2000.

tive (negative) values over much of the Midwest in the summer of 1999 (2000), associated with the satellite viewing more often the warmer land surface (colder cloud tops). These OLR spatial patterns are consistent with the NNR total cloud amount maps for the same periods (not shown), and with the seasonally averaged precipitable water (PW) anomalies (Figs. 3a,b) and relative humidity (RH) mean anomalies for the lower-to-midtroposphere (Fig. 3c): the summer of 1999 was characterized by negative anomalies of atmospheric moisture, which is mostly positive in 2000. These contrasting anomaly patterns of PW and RH(700) resemble the seasonally averaged anomalies of vertical motion, or omega, such that in the summer of 1999 subsiding air at 700 hPa promoted drying (Fig. 3c), whereas in the following summer, the Midwest was dominated by ascent and potential moistening of the air (Fig. 3d). Overall midtropospheric height anomalies were positive and had associated weaker gradients in 1999 (Fig. 3e); in 2000, stronger gradients were located between positive (negative) anomalies in western (eastern) parts of the Midwest larger region (Fig. 3f).

Certain summer-averaged tropospheric fields show relatively little difference between 1999 and 2000. In particular, the mid-to-upper-tropospheric zonal wind (i.e., u component) over the CCB was broadly similar: u(500) anomalies were close to zero in the summer of 1999, and only slightly stronger in 2000 (Figs. 3e,f). The orientation and tighter gradients of Z(500) in the summer of 2000 (Fig. 3f) imply an enhanced meridional

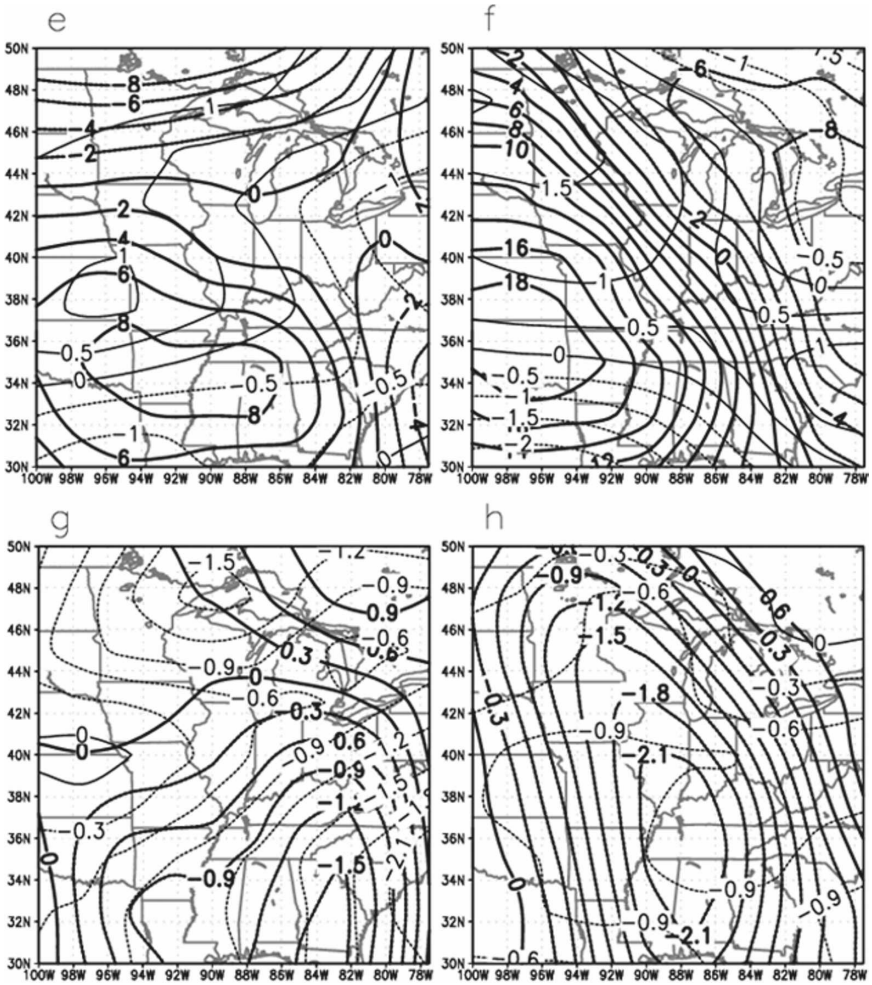

FIG. 3. (*Continued*)

component of the wind; specifically, stronger northerlies [e.g., $v(700)$, cf. Figs. 3g,h]. In 1999, the Upper Midwest experienced light southerly anomalies, apparently connected with the LLJ over the central and southern plains. Many authors (e.g., Hu and Feng 2001; Kunkel and Liang 2005) point out the importance of southerly low-level airflow for summertime rainfall in the central United States. Finally, sea level pressure (SLP) anomalies were negative over most of the Midwest, including the CCB, in both summers (Figs. 3g,h).

3. Research hypothesis, objectives, and approach

a. Hypothesis

To determine the relative influence of synoptic atmospheric circulation and land surface mesoscale conditions on deep convection in the CCB for the contrasting summers of 1999 and 2000, we formulated two separate yet related research hypotheses. Hypothesis 1 is evaluated in the present paper; hypothesis 2 derives from the results of testing hypothesis 1, and is presented and examined in Part II. Radar-indicated deep convection—a proxy for precipitation—tends to be more organized (scattered) for strong (weak) background flow, and the latter variable is linked to the synoptic circulation. Thus, a first-order stratification of the spatial extent and severity of convective storms involves the associated free-atmosphere wind speed (Yan and Anthes 1988; Chen and Avissar 1994b; Lynn et al. 1998; Connor and Woodcock 2000). This is expressed by hypothesis 1, as follows: The presence of radar-indicated deep convection and its morphological type ("organization") for the CCB in a given summer varies by category of vector wind in the mid- and upper troposphere, from being isolated or scattered (i.e., unorganized) on days having weaker flow, to being more organized on days of stronger flow. These differences in convective activity

should manifest, respectively, more barotropic (baroclinic) conditions, evident as increasing spatial synchroneity of synoptic features promoting or representing a strong upward motion of air, with precipitation spatial maxima, as the background wind increases. Moreover, differences (i.e., magnitude and sign) between atmospheric composites for convection versus no-convection days of the same background flow category should increase with increasing wind speed, implying a greater influence of land surface conditions on deep convection for the weaker flow contrasted with stronger flow days.

In Part II, the role of these land surface conditions in the convective precipitation variations of the summers of 1999 and 2000 is examined with respect to the longer period of 1995–2001. Accordingly, in Part I we use a broadly similar period (1996–2001) to provide climatic context for the summers of 1999 and 2000 results of background flow–convective activity associations for the CCB. Both papers utilize a multiday composite approach, which generates spatial patterns by averaging meteorological variables, or their anomalies, from a longer base period, for multiple days or time periods (Higgins et al. 1997; Schubert et al. 1998). As a fundamental technique of synoptic climatology (e.g., Carleton 1999), compositing reduces the influence of an individual event and illuminates the dominant circulation controls (e.g., Chen and Kpaeyeh 1993). The method is most robust when categories are realistically associated with the phenomenon under study (e.g., Walters and Winkler 2001; Bentley and Stallins 2007); here, background flow and convective activity in the CCB. The resulting spatial fields should be readily interpretable by a synoptic analyst or forecaster (e.g., Walters 2001).

b. Objectives

Research hypothesis 1 comprises three objectives, which we evaluate as follows:

1) For the summers of 1999 and 2000, daily convective activity (e.g., occurrence, radar morphological type, etc.) and vector wind speed at 500 hPa [**V**(500)] are characterized for the CCB, and their mutual associations are identified;
2) The results determined in objective 1 are situated climatically by reference to the summer-season averages of background flow and convective activity for the longer period of 1996–2001;
3) Composite daily averaged NNR meteorological anomaly fields and high-resolution precipitation network observations, by **V**(500) and "convection" ("CV") versus "no convection" ("NC") joint categories, are examined separately for 1999 and 2000. Spatially close associations between the synoptic circulation and precipitation composites for a given **V**(500) and convective activity pair that are physically reasonable (i.e., large values of negative omega collocated with precipitation maxima) disclose the dominant role of the top-down climatic control on deep convection in a given study summer; spatial disparities between the two sets of composites (i.e., synoptics, precipitation, etc.) identify likely areas of mesoscale stationary (climatic) influence on deep convection connected to the land surface (examined in Part II).

TABLE 1. Classification of the daily averaged background wind speed, given by the mean spatial ranges of **V**(500) over the CCB for the summers of 1999 and 2000, and the corresponding categories of **V**(300) used to classify the 6 summer seasons 1996–2001. Also shown are the mean spatial ranges of **V**(sfc) for each **V**(500) category (i.e., 1999 and 2000).

	V(500), m s^{-1}	**V**(300), m s^{-1}	**V**(sfc), m s^{-1}
Category	Spatial range 1999 and 2000	Magnitude range of values	Spatial range 1999 and 2000
WF	5–11	<12	1.0–4.0
W-MF	4–12	12–18	1.0–5.0
MF	11–17	18–25	1.0–3.5
MF-J	10–18	25–33	1.5–3.0
J	13–17	>33	1.0–3.5

c. Classificatory approach

1) DETERMINATION OF DAILY BACKGROUND WIND SPEED

To fulfill objectives 1 and 2, we developed two complementary and related measures for classifying daily background flow over the CCB. Specifically for the 1999 and 2000 study summers, and given that the CCB's major axis is oriented west–east—paralleling the typical movement of weather systems in the Midwest—the first measure involves the spatial range of vector wind speed values in the midtroposphere (500 hPa), or **V**(500) (Table 1). Each day's **V**(500) was determined visually as a temporal average of the individual 12-h (i.e., 0000 and 1200 UTC) vector wind spatial ranges, grouped ultimately into the following five nominal categories that represent a more-or-less consistent increase in wind speed: weak flow (WF), weak-moderate flow (W-MF), moderate flow (MF), moderate flow-jet (MF-J), and jet (J). This final five-category classification of **V**(500) was arrived at after experimenting with a three-category classification having broader class intervals (i.e., WF, MF, J); however, a sizeable proportion of days straddled the stronger end of WF and weaker end of MF, and the stronger end of MF and weaker end of J. Accordingly, two "hybrid" categories (i.e., W-MF

and MF-J) were added, each of which has a larger spatial range (i.e., stronger west–east gradient) in **V**(500) than its adjacent primary categories (Table 1), and the classification of days was redone for both summer seasons using the five categories. This procedure classified all days in the 1999 and 2000 summers, except those very few identified as "transitional." Transitional days have nonadjacent categories of **V**(500) for the consecutive synoptic times spanning a 24-h period (i.e., 0000, 1200, and 0000 UTC); for example, J→ MF→ WF. For certain analyses (section 5a), transitional **V**(500) days were included in the statistics by temporally averaging the categories on consecutive maps (MF, in this example); however, extra weight was given to the 0000 UTC map because it is closer to the time of maximum convection due to surface heating. The **V**(500) data for the two study summers (1999 and 2000) are combined in Table 1, given the similarity of u-wind mean anomaly values in the mid-to-upper troposphere (e.g., Figs. 3e,f).

The second measure of background flow for the CCB is the upper-tropospheric (300 hPa) vector wind speed near the jet stream level [**V**(300)], developed to classify all 558 days in the six-summer period of 1996–2001 from the ready availability online of color-coded (by wind speed range) 12-h (0000–1200 UTC) maps (available online at http://weather.unisys.com/archive/eta_init/). The "transfer function" from **V**(500) to **V**(300) involved visually classifying the **V**(300) magnitude range according to that day's **V**(500) category (e.g., WF and MF-J), for the 1999 and 2000 summers. The mean-range classes of **V**(300) shown in Table 1 are the most frequently associated with each **V**(500) category. Because the **V**(300) data are at a higher altitude than those used to develop the **V**(500) classification, the wind is stronger, on average. Moreover, the differences between **V**(500) and **V**(300) increase with increasing wind speed; they are small for category WF and large for J, confirming equivalent barotropic conditions in the midlatitude troposphere (Wallace and Hobbs 1977, their chapter 8.6). There was no association either between the average spatial ranges of wind speed at the earth's surface in the summers of 1999 and 2000 or for the categories of **V**(500) and **V**(300) (Table 1); relatively light surface winds occurred for both WF and J.

2) Determination of daily convective activity

Information on the presence or absence of deep convection (i.e., CV and NC) in the CCB and its generalized morphological signature type for each afternoon and evening combined period in the summers of 1996–2001 (i.e., objectives 1 and 2) was also determined manually. The primary data source comprised Next Generation Weather Radar (NEXRAD) composite images spanning the time of maximum surface heating (e.g., Tian et al. 2005); that is, 1500–0000 UTC or 0900–1800 CST. These images are collated from individual National Weather Service (NWS) Weather Surveillance Radar-1988 Doppler (WSR-88D; National Weather Service 2001) station scans, and are available hourly for most days in the six-summer period (more information is available online at http://www4.ncdc.noaa.gov/cgi-win/wwcgi.dll?WWNEXRAD~Images2). Missing data for the typically small number of days each summer (average = 4 out of 93 days) were filled in using the individual station radar scans at high temporal frequency (more information is available online at http://www.ncdc.noaa.gov/nexradinv/); specifically, those for Davenport, Iowa (KDVN); Lincoln, Illinois (KILX); Indianapolis, Indiana (KIND); and Cincinnati, Ohio (KILN), which provide a west–east transect through the CCB.

Deep convection was generally considered to occur at radar echo intensities around 40 dBZ and higher, and the ability to animate sequences of images online aided in determining convection occurrence and its dominant signature type. The NC days were evident from either the complete absence of echoes or only scattered for very low intensity echoes likely associated with virga. For CV days, key descriptors of the echoes also were recorded (e.g., Jirak et al. 2003), including the generalized intensity (two classes: light to moderate and moderate to heavy), the areal coverage within the CCB (three classes: isolated, scattered, and widespread), and the dominant shape of "organized" echoes, particularly MCSs and QLCSs (Trapp et al. 2005). In subjectively classifying radar-indicated convection according to these nominal descriptors, our aim was not to diagnose physical processes occurring within organized signatures or to attempt to develop mesoscale composites of signature types, but to stratify each day's convective activity consistently as a basis for deriving synoptic atmospheric composites of the summers of 1999 and 2000.

Organized echoes involve five key types gleaned from previous studies of radar echo features in the central U.S. and Corn Belt region (Parker and Johnson 2000; Jirak et al. 2003), and from our perusal of a large number of NEXRAD images for the CCB, as follows: linear narrow (LN), linear wide (LW), MCS-oval (i.e., MCC), MCS-line echo wave pattern (MCS-LEWP), and shield (SH). Convection organized linearly is characterized by a dominant long major axis; narrow squall lines (LN) tend to occur with weaker synoptic forcing and a lack of vertical wind shear than those associated

TABLE 2. NNR variables for which composite maps were generated on multiple nonadjacent days in summer seasons (15 Jun–15 Sep) of 1999 and 2000.

Variable	Level(s)	Units	Temporal resolution	Reliability*
T	Sfc, 850, 700, 500	°C	Daily avg	B (sfc), A
SLP	Sfc	Pa	Daily avg	A
Z	1000, 850, 700, 500	m	Daily avg	A
Layer thickness	1000–500	m	Daily avg	A
v	700	m s^{-1}	Daily avg	A
u	500, 300	m s^{-1}	Daily avg	A
$\mathbf{V}$	1000, 850, 700	m s^{-1}	Daily avg	B (1000), A
q	1000, 850, 700	g kg^{-1}	Daily avg	B
PW	Sfc.	kg m^{-2}	Daily avg	B
OLR	TOA**	W m^{-2}	Daily avg	C
$\omega(= dp/dt)$	Sfc, 700	Pa s^{-1}	6 h, daily avg	B
SLI	Sfc	°C	6 h	B
BLI	Sfc–500	°C	6 h	B

* Reliability classes according to Kalnay et al. (1996, their appendix A), where reanalysis A variables are strongly influenced by observations, B variables are influenced by both observations and the model, and C variables are entirely model derived.
** Top-of-the-atmosphere value.

with wide squall lines (LW). The latter may accompany cold fronts and jet stream maxima (Houze 2004). Accordingly, LN features tend to be shorter lived than LW. Convection organized nonlinearly as an oval shape (i.e., MCC) possesses a longer minor axis than that of QLCSs. These features occur in environments of strong warm-air advection, commonly involving a southerly LLJ, where low-level convergence is enhanced along meso- or synoptic-scale atmospheric boundaries that accompany moderate-to-strong upper-level divergence and vertical wind shear (Maddox 1980; Smull and Augustine 1993). The MCS-LEWP signature is a mesoscale wavelike feature that develops in response to convergence of unstable air along quasi-linear boundaries accompanying strong vertical wind shear. Two subclasses are the serial and progressive LEWP systems (Davis and Trier 2002; Davis et al. 2004) involving, respectively, systems generally exhibiting greater latitudinal extent (for north–south-oriented features), and those revealed as "comma-shaped" radar signatures that propagate orthogonally to the near-surface atmospheric boundary. The MCS-shield (SH) system tends not to exhibit a "bowing" radar signature—which would otherwise indicate greater intensity (Weisman 1993)—and is slower moving than the MCS-LEWP type. The SH feature is associated with an upshear slope to the convective updrafts, resulting in a wide stratiform precipitation region immediately following the dominant leading edge (Yu et al. 1999).

4. Synoptic circulation and precipitation data and their analysis

Fulfillment of research objective 3, using the above-described approaches, requires datasets at both synoptic and meso-spatial scales; respectively, the daily-averaged NNR maps and point-location precipitation once-daily reports.

a. NCEP–NCAR reanalyses (NNR)

The NNR composes the primary data source for the composite meteorological fields (objective 3; Kalnay et al. 1996; Kistler et al. 2001; also available online at http://www.cdc.noaa.gov/). These data have been used in previous studies depicting atmospheric signatures of interannual climate variations for the central United States (e.g., Hu and Feng 2001; Oglesby et al. 2001; Sudradjat et al. 2003). The NNR spatial scale is commensurate with circulation climate controls and their variability (e.g., Dominguez and Kumar 2005), and can capture features such as southerly LLJs (Anderson and Arritt 2001; Byerle and Paegle 2003). For each summer (i.e., 1999 and 2000) and each NNR variable, we compute map composites of the daily averaged anomalies from the long-term daily means stratified by $\mathbf{V}(500)$ and the convective activity joint classes.

In Table 2, we consider some variables [e.g., geopotential height at 500-hPa $Z(500)$, $u(300)$, and omega(700)] to be "dynamic variables" because these pertain to forcing of vertical motion fields, whereas others [e.g., surface lifted index (SLI) and the "surface omega" $T(\text{sfc})$] pertain more directly to the earth's interactions with the PBL (i.e., "thermodynamic variables"). Here, we emphasize the dynamic variables as they portray synoptic circulation associations with deep convection and precipitation; thermodynamic variables are examined in Part II.

To minimize the influence of a run of days classified

as the same **V**(500) category (i.e., temporal autocorrelation problem), we only use one date per sequence when generating composites. For a run of 2 days, the included day is the one deemed more representative of the flow type; for a run of 3 days, the central day is used. The same procedure is adopted for compositing the precipitation data (sections 4b and 5b). The domain for compositing NNR data (30°–50°N, 100°–77°W; Fig. 5) encompasses the Midwest larger region (Fig. 1), and with the CCB located just downstream (i.e., east) of the grid center. The latter accommodates the general west–east movement of synoptic systems that occurs in the region, even in summer (Elliott 1949; Schubert et al. 1998; Carbone et al. 2002).

b. *Station precipitation*

Precipitation data at "subgrid scales" (Nykanen et al. 2001; Gutowski et al. 2003) are available within the DSI-3200 dataset (NCDC 2003), and comprise observations from approximately 23 000 cooperative, automated, military, and first-order observing sites from 1948 to the present; the bulk of which are cooperative. Personnel at NCDC have applied stringent quality control to the observations, including checks for internal consistency and temporal homogeneity, and by comparing data with those at surrounding stations. The DSI have been used extensively in climate studies and to evaluate model simulations (e.g., Brown et al. 2003; Hu and Feng 2003; Kunkel and Liang 2005), sometimes with customized adjustments (e.g., Kunkel et al. 1998).

At most NOAA/NWS cooperative stations, precipitation observations are taken either at 0700 or 1900 LT, and represent the total amount for the preceding 24 h. For the study summers of 1999 and 2000, we used those stations recording observations at 0700 LT (+/−2 h) because this includes precipitation derived from the heating maximum of the previous afternoon and early evening (cf. Segal and Arritt 1992). Composites derived using the 1900 LT observations would not include all the convective precipitation of that day, but would include precipitation from the previous late evening; more than likely for a different background flow category. Applying the aforementioned selection rules, data from approximately 1300 stations were used to compute composite maps of precipitation mean amounts and their standardized anomalies—calculated as spatial departures from the mean value of precipitation for the larger Midwest region on all days in each summer, according to joint **V**(500) and CV/NC categories. The precipitation observations were interpolated into 1° × 1° latitude–longitude grid cells by a geographic information system (GIS) to reduce the spatial aliasing typically associated with convective precipitation, and differences from the overall mean for each grid cell were determined. This procedure permits the spatial relationships of precipitation to be determined for each **V**(500) category irrespective of differences in station spatial density. Composites (i.e., multiday average) analysis of Midwest precipitation data at relatively high spatial resolutions should reveal distinct subregional-scale patterns (cf. Richman and Lamb 1985).

5. Results

a. *Synoptic context of the 1999 and 2000 summer seasons*

1) BACKGROUND FLOW REGIMES, CONVECTIVE ACTIVITY, AND THEIR COASSOCIATIONS

Frequencies of the five background flow categories for the CCB (Fig. 1) in the study seasons of 1999 and 2000 are placed in context of summers in the period of 1996–2001 (Table 3). For the six summers combined (Table 3a), the frequencies are broadly Gaussian: highest frequencies occur for the MF category, or **V**(300) approximately 18–25 m s^{-1}, with the two end categories (i.e., WF and J) having the lowest frequencies. Subtracting the multisummer **V**(500) category averages from the normalized totals for the study seasons of 1999 and 2000 (Table 3b) shows that WF and jet were enhanced relative to the middle categories (i.e., W-MF, MF, and MF-J) in both years. Thus, in terms of background flow regime, the summers of 1999 and 2000 appear more similar to each other than does either one to the multisummer averages. Clearly, a fuller explanation for the anomalies in circulation climate and precipitation for the CCB between the summers of 1999 and 2000 (Figs. 2 and 3) requires variables additional to an index of background wind speed.

Figure 4 stratifies convection occurrence (i.e., CV) and nonoccurrence (i.e., NC) by **V**(500) category for each of the two study summers. Comparing frequencies within a given summer indicates that convection most often was associated with WF in 1999, secondarily with MF; convection occurred less frequently for the two hybrid categories. In summer 2000, CV days were distributed more evenly across **V**(500) categories, having the greatest frequency for the W-MF type; secondarily for J and MF. The frequencies of NC days also differed by the **V**(500) category for a given summer (Fig. 4); for example, MF-J (in 1999) was the only category for which the number of NC days appreciably exceeded the CV days.

As a context for the results shown in Fig. 4, Table 4 gives frequencies of afternoon and evening deep convection (CV) in, and its absence (NC) from, the CCB

TABLE 3. Summer-season totals (per 93 days) and normalized frequencies (per 100 days, or %; italicized in parentheses) of background flow by (a) **V**(500) categories for 1996–2001 and departures of the (b) 1999 and (c) 2000 summer frequencies from the all-summer means.

(a) Category of **V**(500)						
Yr	WF	W-MF	MF	MF-J	J	Transitional
1996	6 (*6.5*)	32 (*34.4*)	29 (*31.2*)	15 (*16.1*)	11 (*11.8*)	0 (*0*)
1997	2 (*2.1*)	30 (*32.3*)	34 (*36.6*)	20 (*21.5*)	7 (*7.5*)	0 (*0*)
1998	7 (7.5)	23 (24.7)	32 (34.4)	24 (25.8)	7 (7.5)	0 (*0*)
1999	29 (*31.2*)	9 (*9.7*)	21 (*22.6*)	12 (*12.9*)	21 (*22.6*)	1 (*1.1*)
2000	15 (*16.1*)	20 (*21.5*)	22 (*23.7*)	11 (*11.8*)	23 (*24.7*)	2 (*2.1*)
2001	8 (*8.6*)	25 (26.9)	27 (*29.0*)	26 (*28.0*)	7 (*7.5*)	0 (*0*)
(b)						
Mean 1996–2001	11.1 (*12.0*)	23.2 (*24.9*)	27.5 (*29.6*)	18.0 (*19.3*)	12.7 (*13.6*)	0.5 (*0.5*)
Mean 1996–98, and 2001	5.7 (*6.2*)	27.5 (*29.6*)	30.5 (*32.8*)	21.3 (*22.9*)	8.0 (*8.6*)	0 (*0*)
(c)						
1999 minus mean 1996–2001	+17.9 (+*19.2*)	−14.2 (−*15.2*)	−6.5 (−*7.0*)	−6.0 (−*6.5*)	+8.3 (+*9.0*)	+0.5 (+*0.6*)
2000 minus mean 1996–2001	+3.9 (+*4.2*)	−3.2 (−*3.4*)	−5.5 (−*5.9*)	−7.0 (−*7.5*)	+10.3 (+*11.1*)	+1.5 (+*1.6*)

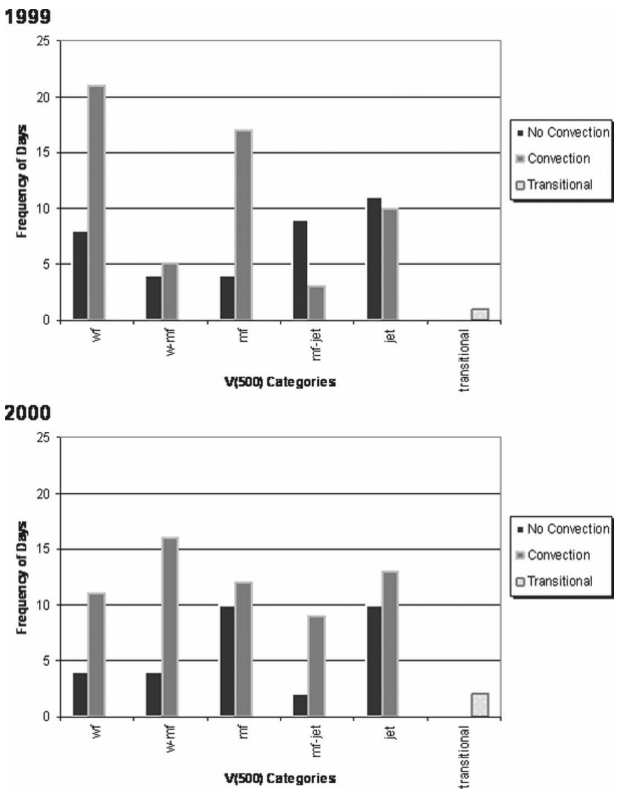

FIG. 4. Frequencies of days in each summer (15 Jun–15 Sep) classified by categories of average vector wind speed at 500 hPa [**V**(500)]—refer to Table 1—and by CV vs NC occurrence for the CCB (refer to Fig. 1): (a) 1999 and (b) 2000. Transitional days are defined as having nonadjacent categories of **V**(500) for at least two of the three consecutive synoptic times (0000, 1200, and 0000 UTC) in a 24-h period.

for the summers of 1996–2001. An additional category (transitional) accommodates the relatively small number of days in a typical summer (<4%) for which convection in the CCB either occurred late in the evening (i.e., NC → CV), or no-convection conditions replaced convection during the peak afternoon hours of heating (i.e., CV → NC). For the six-summer period, the ratio of CV to NC days is around 3:2. Expressing the summers of 1999 and 2000 normalized frequencies in each of the three categories as departures from the multi-summer averages (Table 4) confirms that convection-day frequencies were reduced in 1999 and increased in 2000 (Fig. 4), but with additional features also evident:

TABLE 4. Summer-season totals (per 93 days) and normalized frequencies (per 100 days, or %; italicized in parentheses) of CV, NC, and transitional (CV → NC and NC → CV) days, determined from manual interpretation of NEXRAD data for the CCB during the summers of 1996–2001.

Convective activity class			
Yr	CV	NC	Transitional
1996	54 (*58.1*)	32 (*34.4*)	7 (*7.5*)
1997	48 (*51.6*)	43 (*46.2*)	2 (*2.2*)
1998	59 (*63.4*)	31 (*33.3*)	3 (*3.2*)
1999	55 (*59.1*)	32 (*34.4*)	6 (*6.5*)
2000	62 (*66.7*)	30 (*32.2*)	1 (*1.1*)
2001	58 (*62.4*)	33 (*35.5*)	2 (*2.2*)
Mean 1996–2001	56.0 (*60.2*)	33.5 (*36.0*)	3.5 (*3.8*)
Std dev	4.43 (*4.78*)	4.35 (*4.68*)	2.22 (*2.38*)
1999 minus mean 1996–2001	−1.0	−1.5	+2.5
2000 minus mean 1996–2001	+6.0	−3.5	−2.5

TABLE 5. Joint frequency distributions of background flow [**V**(500) category] and convective activity (i.e., CV and NC) for the summers during 1996–2001, given as the total number of days for the six summer seasons (regular font) and the mean frequency per summer (in italics), and departures of the 1999 and 2000 normalized frequencies from the all-summer means.

	Background flow category					
Activity	WF	W-MF	MF	MF-J	J	Σ (*mean*)
CV	48 (*8.0*)	88 (*14.7*)	105 (*17.5*)	67 (*11.2*)	42 (*7.0*)	350 (*58.3*)
NC	18 (*3.0*)	52 (*8.7*)	61 (*10.2*)	43 (*7.2*)	34 (*5.7*)	208 (*34.7*)
1999 minus 1996–2001	WF	W-MF	MF	MF-J	J	Σ
CV (diff)	20.7 (+12.7)	5.9 (−8.8)	17.8 (+0.3)	4.9 (−6.3)	8.9 (+1.9)	58.2 (−0.1)
NC (diff)	7.1 (+4.1)	4.1 (−4.6)	3.1 (−7.1)	8.2 (+1.0)	12.3 (+6.6)	34.8 (+0.1)
2000 minus 1996–2001	WF	W-MF	MF	MF-J	J	Σ
CV (diff)	10.3 (+2.3)	15.1 (+0.4)	11.3 (−6.2)	9.4 (−1.8)	12.2 (+5.2)	58.3 (0.0)
NC (diff)	4.5 (+1.5)	4.5 (−4.2)	12.3 (+2.1)	2.2 (−5.0)	11.2 (+5.5)	34.7 (0.0)

although the greater frequency of convection days in the "moist" summer of 2000 exceeds the one standard deviation value for the six-summer period, the percent decrease in convection days for the "dry" summer of 1999 is well within the standard deviation for the multisummer period. Moreover, there is a small decrease in NC days for the summer of 1999, which was not expected; interestingly, this summer had the second highest frequency of convective transitional days (Table 4). These results indicate that the radar-determined presence or absence of afternoon and evening deep convection within the CCB is a useful stratification approach and suggests additional years that might fruitfully be analyzed (e.g., 1997). However, this measure alone does not explain the large precipitation differences between summers, which should be analyzed for their coassociations with the background wind.

In evaluating the six-summer average joint distributions of background flow [i.e., **V**(500) categories] and deep convection for the CCB, we reclassified the relatively few convective transition days (i.e., CV → NC and NC → CV) into, respectively, NC and CV. The summer-season mean results (Table 5) confirm Tables 3 and 4: convection is most likely with moderate flow (MF) conditions (17.5 days per summer), and least likely for both WF (8 days per summer) and jet (7 days per summer) conditions. Although most NC days also occur with MF (average of 10 days per summer), by far the fewest NC days occur with WF (3 days). The latter result may indicate a land surface influence on deep convection when the background wind speed is slow, a possibility that is explored further in section 5e and in Part II. Differences between the mean frequencies of CV and NC days are smallest for the category of strongest winds in the upper troposphere (i.e., J): convection and no convection are almost equally as likely when **V**(300) exceeds approximately 30 m s^{-1}. The physical reasons for this result are made clear in section 5b(2).

Differencing the individual summer (i.e., 1999 and 2000) joint frequencies of background wind and convection presence or absence from the six-season mean values (Table 5) confirms that convection was enhanced for both the slowest (i.e., WF) and fastest (i.e., J) categories of **V**(500) in both years, yet reduced for most of the intermediate categories. In the summer of 1999, the biggest increase in convection relative to the six-summer averages occurred with WF (i.e., +13 days), while the adjacent category (i.e., W-MF) showed a decrease of almost 9 days (cf. Fig. 4). In the summer of 2000, the biggest increase in convection occurred for category J (i.e., + 5 days), although it was still enhanced relative to the six-summer means for both WF and W-MF. The NC-day frequencies similarly were enhanced for the extreme background flow categories (i.e., WF and J) in both 1999 and 2000. As was also noted from Tables 3 and 4, the summers of 1999 and 2000 were more similar to each other in terms of background flow and convection occurrence than they were to the longer-term (1996–2001) summer averages of these indices (Table 5). Again, reasons for the precipitation differences in the CCB for these two summers in terms of atmospheric circulation should be sought in measures that go beyond a relatively simple index of background wind speed (see section 5d), and should also consider the convection morphological type.

2) RADAR SIGNATURE ASSOCIATIONS WITH BACKGROUND FLOW

The daily level information on radar convective signature types [see section 3c(2)] reveals mean associations with background flow for the six summer seasons (Table 6) and permits determination of differences for the 1999 and 2000 summers (Table 7). For statistical testing, and to maintain adequate cell frequencies across **V**(500) categories, three logical groupings of

TABLE 6. Joint frequency distributions of NEXRAD-indicated convective morphology signatures (three groups: unorganized, organized linear, and organized nonlinear) and background flow categories during the summers of 1996–2001. Cell values in regular font are raw totals for the six summers; cell values in parentheses are seasonal means normalized to the mean number of convection days per summer (= 58.3); italicized cell values are normalized frequencies per 100 days (i.e., %). The χ^2 of raw totals = 20.64 ($p < 0.01$ level; significant at >99% confidence level; p(critical) = 20.09 for 8 degrees of freedom).

	Background flow category					
Signature group	WF	W-MF	MF	MF-J	J	Σ
Nonorganized	25 (4.2) *7.1*	37 (6.2) *10.6*	44 (7.3) *12.6*	24 (4.0) *6.9*	14 (2.3) *4.0*	144 (24.0) *41.1*
Organized, linear	15 (2.5) *4.3*	30 (5.0) *8.6*	42 (7.0) *12.0*	20 (3.3) *5.7*	25 (4.2) *7.1*	132 (22.0) *37.7*
Organized, nonlinear	8 (1.3) *2.3*	21 (3.5) *6.0*	19 (3.2) *5.4*	23 (3.8) *6.6*	3 (0.5) *0.9*	74 (12.3) *21.1*
Σ	48 (8.0) *13.7*	88 (14.7) *25.1*	105 (17.5) *30.0*	67 (11.1) *19.1*	42 (7.0) *12.0*	350 (58.3) *100*

convection signature morphology types were formed, as follows: 1) nonorganized: isolated, scattered, and widespread; 2) organized quasi linear: LN and LW; and 3) organized nonlinear: MCC, MCS-LEWP, and SH. On average (Table 6), nonorganized convection in the CCB averaged 24 days per summer season (i.e., 41% of CV days, or 26% of all days); organized linear convection occurred on 22 days (i.e., 38% of CV days, 24% of all days), and organized nonlinear convection occurred on 12 days (i.e., 21% of CV days, 13% of all days). Moreover, the WF category is more likely to have associated nonorganized convection than organized convection; for moderate flow (MF), nonorganized and organized linear radar signatures are about equally likely to occur; and for the jet maximum (J), organized linear convection is the most likely group. This result is reasonable physically, as baroclinity increases with increasing background wind speed (Weisman and Klemp 1984; Rotunno et al. 1988; Johns and Doswell 1992; Parker 2004). The highest frequency of organized nonlinear convection (almost 4 days per summer) occurs for the MF-J category, although frequencies exceeding 3 days also occur for this convection signature group on W-MF and MF days. A chi-squared (χ^2) test of the cell raw frequencies (Table 6) confirms statistical significance at greater than the 0.01 level, thus also validating the manual classification of convection signatures and **V**(500) into the categories so developed. Increasing by 1 the degrees of freedom in Table 6—to accommodate the one cell frequency less than 5—still gives statistical significance at the >0.05 level (i.e., critical value = 16.92). Moreover, including the NC-day frequencies by the **V**(500) category into Table 6 (not shown) gives statistical significance at better than the 0.02 level.

The question of radar signature-type differences of the summers of 1999 and 2000 from the 6-yr totals and averages (Table 6) is particularly relevant given the earlier observation that the dry summer (1999) had a normalized frequency of convection days close to the six-summer average (Table 5), and only 3 days fewer than the normal-to-moist summer of 2000. For WF days in 1999 (Table 7a), the frequency of nonorganized convection exceeded by almost 9 days that having

TABLE 7. Joint frequency distributions of NEXRAD-indicated convective morphology signatures (three groups: unorganized, organized linear, and organized nonlinear) and background flow categories for the summers of (a) 1999 and (b) 2000 and their departures from the six-summer seasonal means (Table 6). Cell values in regular font are raw totals; italicized cell values in parentheses are normalized to the mean number of convection days for the six-summer period (= 58.3).

(a) 1999	Background flow category					
Signature group	WF	W-MF	MF	MF-J	J	Σ
Nonorganized	13 (*12.9*) +8.7	1 (*1.0*) −5.2	9 (*8.9*) +1.6	0 (*0.0*) −4.0	2 (*2.0*) −0.3	25 (*24.7*) +0.7
Organized, linear	5 (*4.9*) +2.4	3 (*3.0*) −2.0	5 (*4.9*) −2.1	2 (*2.0*) −1.3	7 (*6.9*) +2.7	22 (*21.7*) −0.3
Organized, nonlinear	3 (*3.0*) +1.7	2 (*2.0*) −1.5	4 (*3.9*) +0.7	3 (*3.0*) −0.8	0 (*0.0*) −0.5	12 (*11.9*) −0.4
Σ	21 (*20.8*) +12.8	6 (*5.9*) −8.8	18 (*17.8*) +0.3	5 (*4.9*) −6.2	9 (*8.9*) +1.9	59 (*58.3*) 0.0
(b) 2000	Background flow category					
Signature group	WF	W-MF	MF	MF-J	J	Σ
Nonorganized	4 (*3.8*) −0.4	4 (*3.8*) −2.4	5 (*4.7*) −2.6	2 (*1.9*) −2.1	6 (*5.6*) +3.3	21 (*19.8*) −4.2
Organized, linear	4 (*3.8*) +1.3	6 (*5.6*) +0.6	4 (*3.8*) −3.2	3 (*2.8*) −0.5	6 (*5.6*) +1.4	23 (*21.6*) −0.4
Organized, nonlinear	3 (*2.8*) +1.5	6 (*5.6*) +2.1	3 (*2.8*) −0.4	5 (*4.7*) +0.9	1 (*0.9*) +0.4	18 (*16.9*) +4.6
Σ	11 (*10.3*) +2.3	16 (*15.1*) +0.4	12 (*11.3*) −6.2	10 (*9.4*) −1.7	13 (*12.2*) +5.2	62 (*58.3*) 0.0

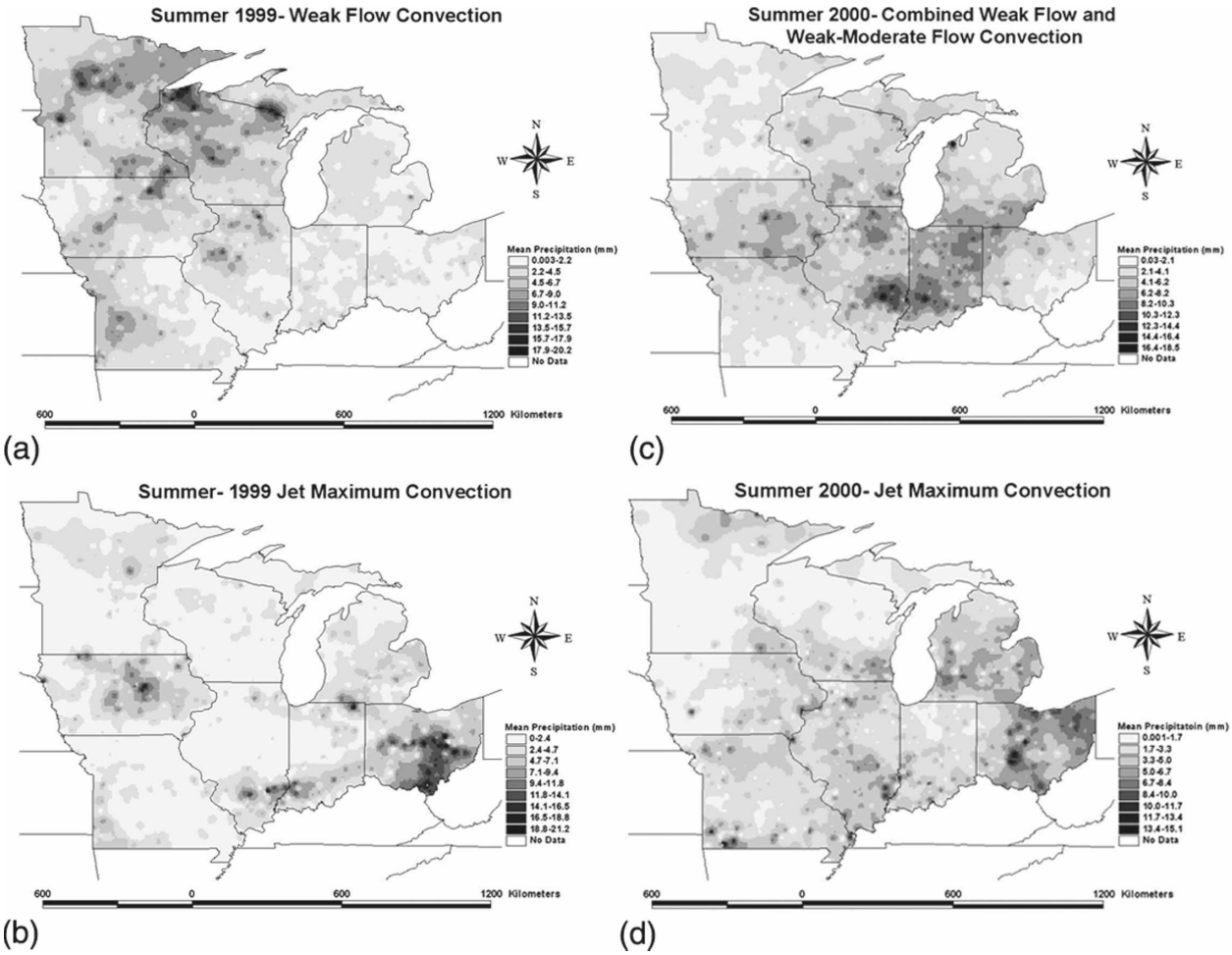

FIG. 5. As in Fig. 2, but stratified by CV days and **V**(500) categories, as follows: (a) 1999 WF, (b) 1999 J, (c) 2000 W+W-MF, and (d) 2000 J.

organized (i.e., linear and nonlinear) convection; for category J, organized linear convection was above the six-summer average by almost 3 days. Conversely, organized nonlinear convection signatures occurred less frequently than the six-summer values for W-MF, MF-J, and J. In the summer of 2000 (Table 7b), nonorganized convection was below the six-summer average for all categories of **V**(500) except J (i.e., + >3 days), while the incidence of organized nonlinear convection mostly increased: these departures (i.e., nonorganized convection and organized nonlinear convection) were greatest for the W-MF category. Thus, the differences between summers of 1999 and 2000 in the CCB are most apparent in their respective frequencies of convection radar signature and background wind joint types: the summer of 1999 saw increases in nonorganized convection for the slowest background wind categories and decreases in organized convection for the stronger wind categories; the summer of 2000 saw more or less the opposite pattern.

The above findings [sections 5a(1), (2)] have the following implications for the present observational analysis of top-down and bottom-up climate controls in the CCB for the summers of 1999 and 2000: 1) The two study summers are confirmed to be different from one another, but also with respect to the six-summer averages (1996–2001) of background flow frequencies and radar-indicated deep convection; 2) the manual approach to classifying both background flow and the combined afternoon and evening deep convection from interpretation of radar morphological signature types, statistically differentiates convective activity from a lack of such activity at the daily level, and highlights their coassociations; and 3) notwithstanding the implication in 2), additional synoptic meteorological variables (e.g., atmospheric moisture and vertical motion),

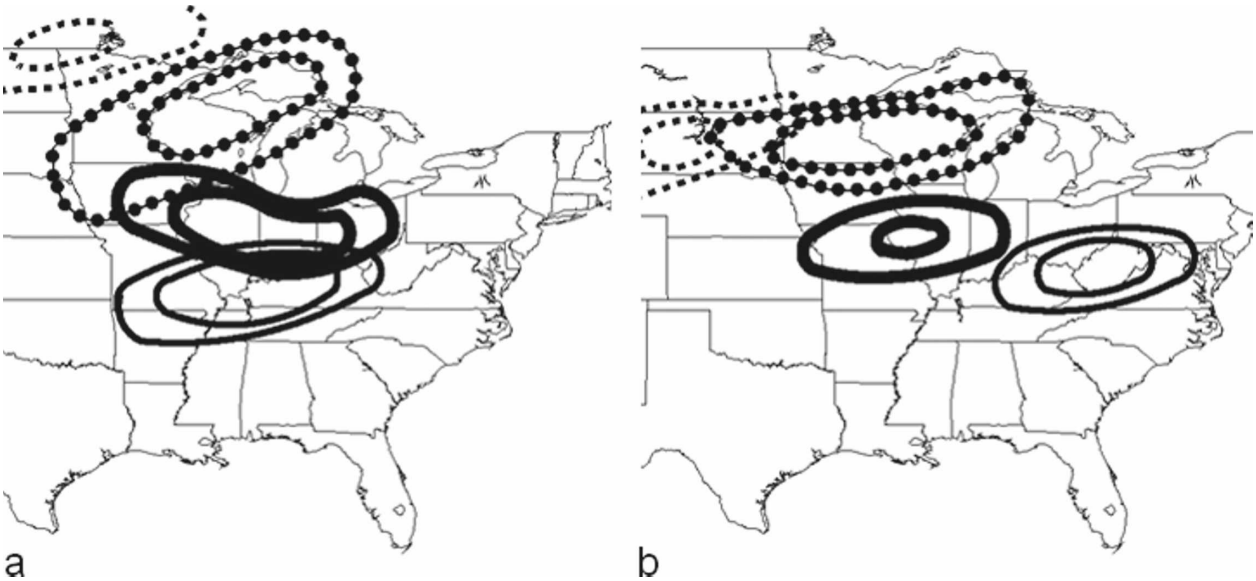

FIG. 6. Locations of composite maxima in the $u(300)$ anomaly field (i.e., isotachs enclosing the strongest westerly wind component) for the following **V**(500) categories determined for the CCB: WF/CV (dashed-line ellipses), MF/CV (chain-line ellipses), J/CV (solid-thick line ellipses), J/NC (solid-thin line ellipses): (a) summer 1999 and (b) summer 2000.

along with consideration of the spatial variations in precipitation, are required to more fully explain the climatic differences between the summers of 1999 and 2000.

b. *Role of synoptic atmospheric conditions in deep convection during the summers 1999 and 2000*

1) PRECIPITATION COMPOSITED BY **V**(500) CATEGORIES

Visual comparisons of spatial relationships between radar-indicated afternoon and evening convection (i.e., CV) and precipitation (following morning observations) are shown (Fig. 5) for the categories of background wind speed (i.e., WF and J) that show marked increases over the six-summer averages (Table 5); for the summer of 2000, WF and W-MF are combined to increase the sample size. In summer 1999, the spatial dipole between the CCB (dry) and the Upper Midwest (wet) was most closely associated with the WF category (cf. Figs. 2a and 5a). However, the classification of daily background flow pertains to the CCB; synoptic regimes are not necessarily the same for the larger Midwest region (e.g., Richman and Lamb 1985). This is confirmed by Fig. 6a, showing the positive anomaly composite centers of u wind at 300 hPa [$u(300)$], or the jet stream maxima, for primary **V**(500) categories in the summer of 1999. Days classified as WF/CV for the CCB had a jet maximum located in the Upper Midwest; thus, the area of heaviest precipitation was located on the jet's southern side in that subarea (Fig. 5a), consistent with dynamical theory and synoptic experience (Uccellini and Johnson 1979; Cammas and Raymond 1989; Bluestein 1993, his chapter 2.8). As **V**(500) increased in the CCB (i.e., MF/CV and J/CV in Fig. 6a), the southward movement of the jet meant that the areas of greatest precipitation shifted into the study area (cf. Figs. 5b and 6a).

In the summer of 2000, the **V**(500) category most closely associated with the area of greatest precipitation in southern Illinois and Indiana (Fig. 2b) is that classified for the CCB and extending just southward; that is, the combined WF and W-MF categories (Fig. 5c). On jet maximum convection days (i.e., J/CV; Fig. 5d), the areas of greatest precipitation were shifted well eastward into Ohio, associated dynamically with the area of most positive $u(300)$ anomaly located just upstream (i.e., westward) on these days (Fig. 6b).

2) COMPOSITE SYNOPTIC CIRCULATION FEATURES ASSOCIATED WITH CONVECTION AND NO CONVECTION

The results in section 5a suggested that determination of the synoptic conditions giving rise to the contrasting patterns of precipitation in the summers of 1999 and 2000, could be achieved with an analysis of dynamic variables additional to the background wind speed. Figures 7 and 8 schematically depict the NNR composite circulation anomaly features that accompa-

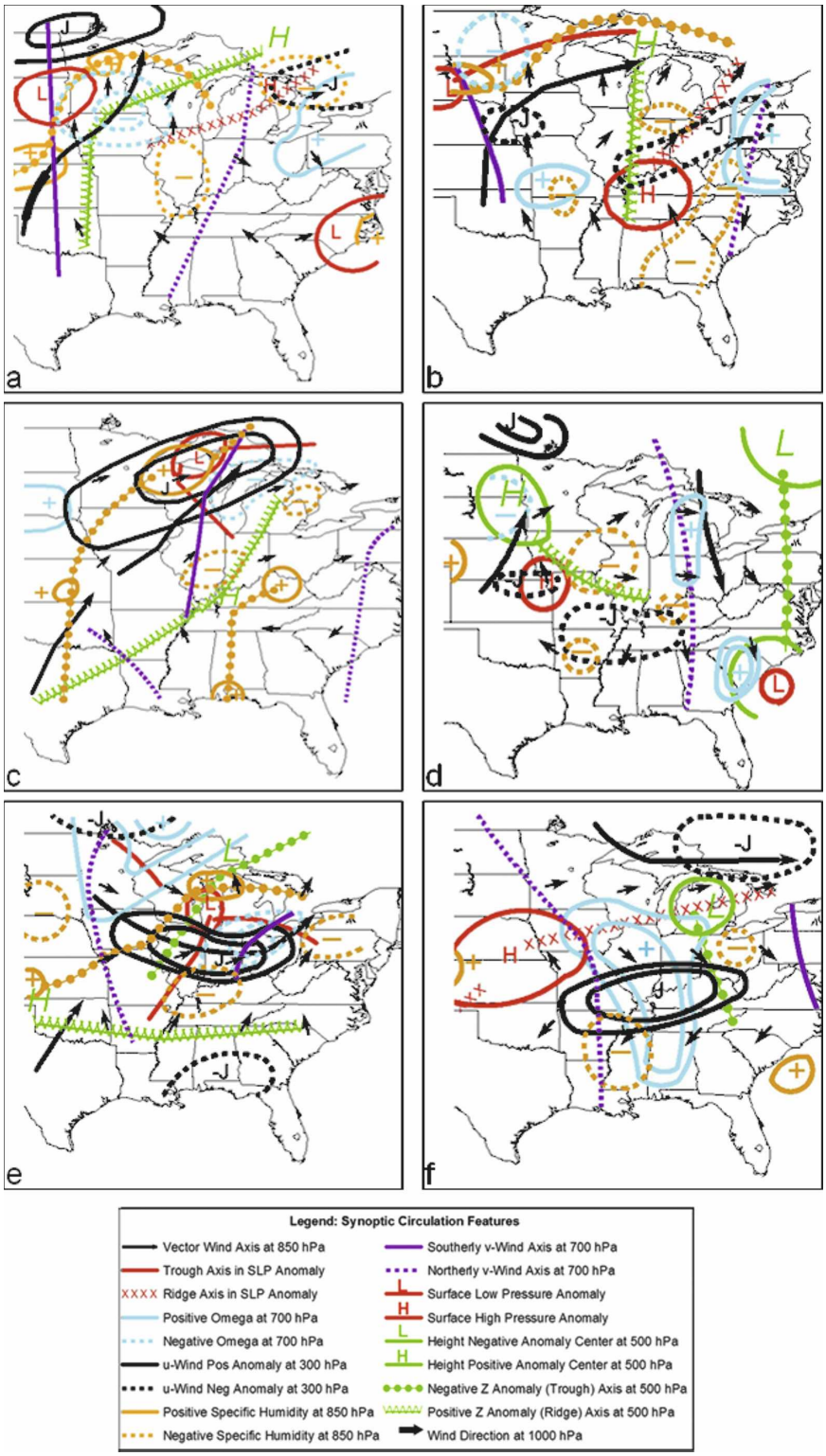

FIG. 7. Summer 1999 schematics of synoptic circulation anomaly features (from composites of NNR daily averaged data), stratified by primary **V**(500) categories and convection occurrence (CV, NC), as follows: (a) WF/CV, (b) WF/NC, (c) MF/CV, (d) MF/NC; (e) J/CV, and (f) J/NC. Refer to legend for symbolization and text for details.

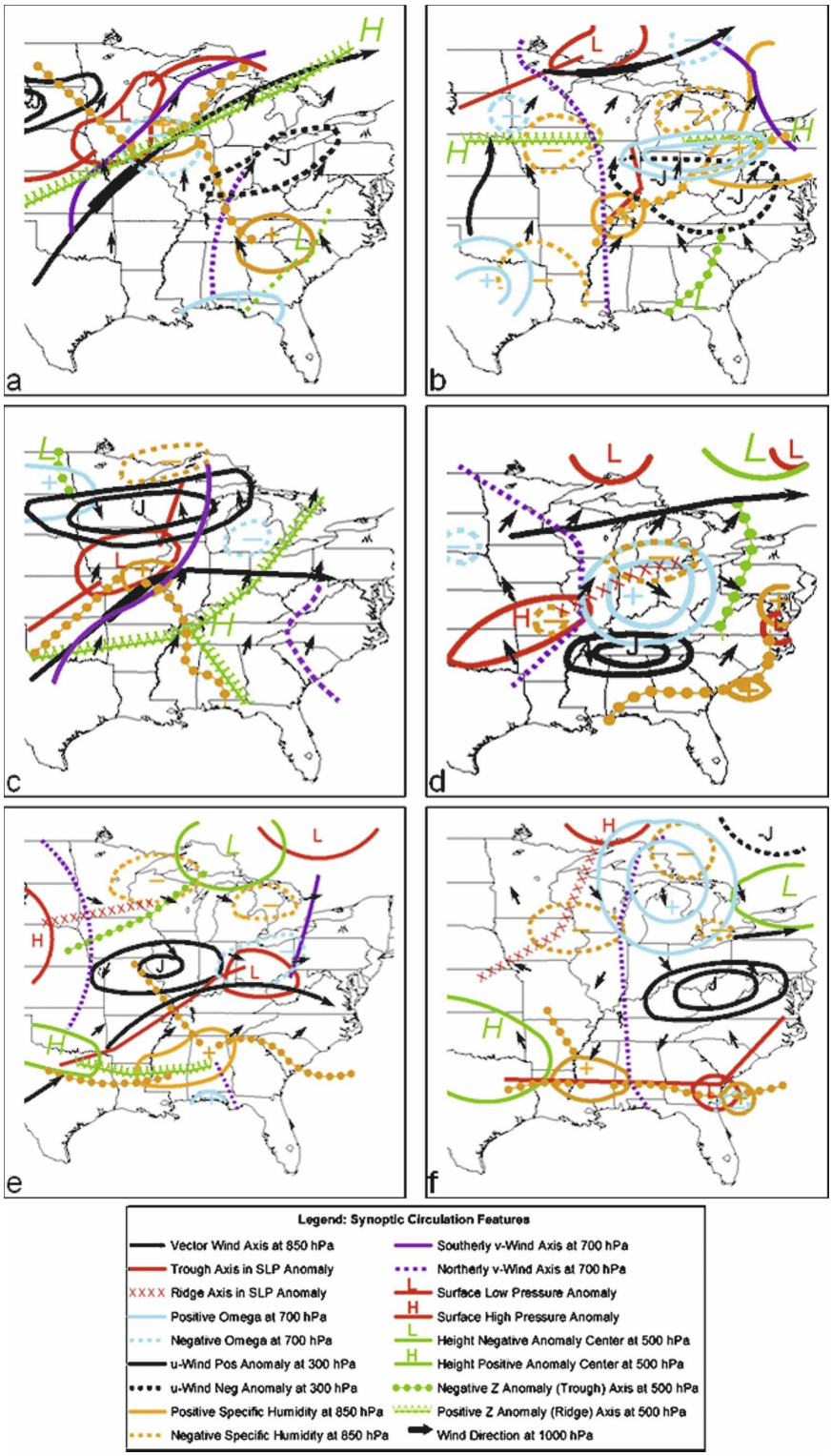

FIG. 8. As in Fig. 7, but for the summer of 2000.

nied radar-indicated deep convection in (i.e., CV), and its absence from (i.e., NC), the CCB in each summer for the primary categories of **V**(500). Similar figures derived for the hybrid **V**(500) categories represent essentially intermediate patterns [e.g., as demonstrated for W-MF (in 1999) in Part II]. In Figs. 7 and 8, different colors pertain to different variables, with positive (negative) anomalies designated as solid (dashed) representative contours. Multiple contours in light blue denote large anomalies of $\omega(700)$; a thickening of the vector wind axis at 850 hPa indicates average speeds exceeding 9 m s^{-1}. For both summers, the synoptic circulation anomaly associations of CV and NC composite days in the CCB can be summarized as follows:

- Convection (no convection) mostly occurred with southerly (northerly) flow in the low-to-midtroposphere. The exception was on WF days, which had southerly flow for both CV and NC composites. On synoptic scales, the propensity for convection on WF days seemed to be determined by the sign and magnitude of the free-atmosphere vertical motion (Figs. 7a,b and 8a,b), consistent with the findings of Portis and Lamb (1988) and Birmingham and Lamb (1994) for the summer precipitation variations in the central United States.
- Negative $\omega(700)$ and rising air [positive $\omega(700)$ and sinking air] was mostly associated with convection (no convection). For CV days these anomalies accompanied low pressure located either to the west or within the CCB; for NC, high pressure or ridging occurred at the earth's surface, aloft, or both (i.e., "warm-cored" high).
- At 850 hPa, a southerly wind maximum was a prominent feature on CV days across all **V**(500) categories. This wind maximum resembles the southerly LLJ of the central United States (Bonner 1968; Mitchell et al. 1995; Higgins et al. 1997; Schubert et al. 1998; Anderson and Arritt 2001; Walters and Winkler 2001), and was located either just west of the CCB (on WF days) or over the area (on MF, J days). Although this LLJ-like feature was sometimes also present in NC composites, it tended to be weaker or discontinuous on those days compared with the corresponding CV composite (cf. Gale et al. 2002). Moreover, some NC composites (e.g., MF/NC in 1999 and J/NC in 1999) showed lower-tropospheric wind maxima consistent with the "northerly LLJs" identified in case studies and short-period climatologies, mostly for the Great Plains (Arritt et al. 1997; Whiteman et al. 1997; Bluestein and Banacos 2002).
- Centers of $u(300)$ positive anomaly on CV days were located either northwest of the CCB (i.e., WF) or over the study region (i.e., MF and J). On WF/NC days there tended to be no such westerly wind maximum in the upper troposphere; when westerly wind maxima were present in the NC composites, these either were located well outside the study area (i.e., MF/NC in 1999), or just to the south (i.e., MF/NC in 2000 and J/NC in 1999 and 2000). For the latter (southward displaced) configuration, the CCB lay beneath the area of negative differential vorticity advection (Carlson 1991, his chapter 4; Moore and VanKnowe 1992) and associated subsidence of air.
- The synoptic-scale baroclinic features promoting upward vertical motion, or negative $\omega(700)$ [i.e., $u(300)$ positive anomaly, surface low pressure and upper trough located to the west, 850-hPa southerly wind maximum, and airmass fronts], were collocated in the CCB on J/CV days (Figs. 7e and 8e). These features were also present on MF/CV days in the summer of 2000, but were less synchronized spatially for this **V**(500) category in the drier summer of 1999. Conversely, on J/NC composite days, subsiding air over the CCB resulted from combinations of the following factors: $u(300)$ anomaly displaced south of the area, the upper low or trough located to the east, and ridging from the west or northwest in the SLP anomaly field (Figs. 7f and 8f). Similar features were also present on MF/NC days in the summer of 2000 (Fig. 8d).

Notwithstanding the above-mentioned broad similarities of synoptic features in both summers on either CV or NC days, there are some interesting differences between years that hint at a contributory land surface influence on deep convection. In the summer of 1999, convection across the primary **V**(500) categories had associated a consistent pattern of specific humidity involving a moisture axis and associated centers of SH(850) positive anomaly located northwest of the CCB, but negative SH(850) over southern parts of the study area (Figs. 7a,c,e). The latter feature coincided with a relative lack of precipitation there, even on CV days (e.g., Figs. 5a,b). Corresponding NC composites (Figs. 7b,d,f) show that negative anomalies of SH(850) either intensified or covered a greater area of the CCB compared with CV days. In the summer of 2000 (Fig. 8), by contrast, days classified as CV (NC) generally showed larger differences in SH(850), especially for MF and J days: positive anomaly centers and moisture axes (negative anomalies) were located over or just west of the CCB. Thus, Figs. 7 and 8 suggest that deep convection in the CCB was organized dynamically on J/CV days in both summers, and on MF/CV days in the summer of 2000; that is, it occurred in the presence of

favorable synoptic conditions. Conversely, convection on WF days (i.e., WF/CV) occurred in the absence of the full suite of favorable synoptic environments, implying additional processes occurring more subtly. On climatic time scales (i.e., the multiday composite over three summer months), these involve the land surface mesoscale influence (Part II). Thus, synoptic-scale factors favoring convection in the CCB (e.g., surface trough, southerly flow near the earth's surface and moisture axis) were present on the WF/NC composite of both years (Figs. 7b and 8b). However, in the summer of 2000 (i.e., WF/NC days), dynamical features unfavorable for convection in the CCB included anomalous northerly wind components [e.g., $\upsilon(700)$ negative anomaly] and strong subsidence of air associated with midtropospheric height positive anomalies. Similarly, days classified as WF/CV (i.e., in 1999) and MF/CV (i.e., in 1999) had associated synoptic conditions in the low-to-midtroposphere that were not highly favorable for convection in the CCB [e.g., $\upsilon(700)$ negative anomaly axis; ridging near the earth's surface and aloft; negative anomalies of moisture at 850 hPa; Figs. 7a,c]. Accordingly, an investigation into other factors likely contributing to convective precipitation on these composite days, particularly subgrid-scale processes associated with land surface–atmosphere interactions, is warranted (Part II).

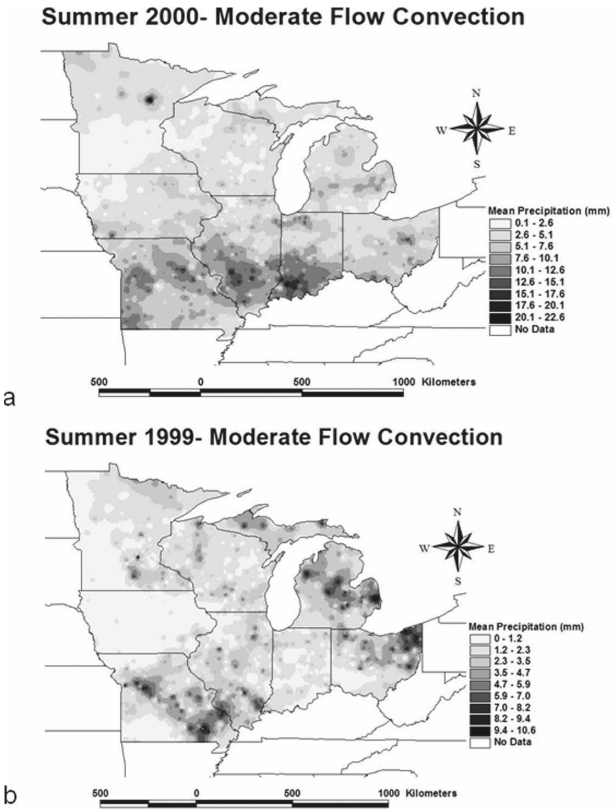

FIG. 9. As in Fig. 5, but for MF/CV days, as follows: (a) summer 2000 and (b) summer 1999.

3) ASSOCIATIONS BETWEEN SYNOPTIC COMPOSITE FEATURES AND PRECIPITATION ANOMALIES BY $\mathbf{V}(500)$

Comparing the synoptic feature schematics for CV days associated with the end categories of $\mathbf{V}(500)$ (Figs. 7a,e and 8a,e) and composite observed precipitation (e.g., Fig. 5) yields further insights into the relationships between synoptic circulation and precipitation in both the larger Midwest and CCB for the summers of 1999 and 2000 (i.e., top-down climate control). On WF/CV days in the summer of 1999 (Fig. 5a), the precipitation positive departures in the Upper Midwest show a spatial synchronization of synoptic features promoting strong upward vertical motion, as follows: intersection of a southerly LLJ and 850-hPa moisture axis over northern Wisconsin and Minnesota, convergence of air into surface low pressure, and location on the south side of the $u(300)$ positive anomaly. Specifically for the CCB, the secondary maxima in precipitation over Illinois (Fig. 5a) are separated from the high-precipitation values in the Upper Midwest and are associated with the following synoptic features not conducive to widespread convection: high pressure and dry air in the lower troposphere; only weak upward vertical motion in the midtroposphere. Conversely, on J/CV days in both 1999 and 2000 (cf. Figs. 7e and 5b; 8e and 5d), stronger precipitation positive anomalies are juxtaposed with most or all of the features denoting baroclinity {i.e., the location near the exit portion of $u(300)$ positive anomaly on the south side of the upper-tropospheric jet, the axis of southerly wind flow [i.e., positive $\upsilon(700)$, LLJ], the moisture axis at 850 hPa, the maximum in the upward vertical motion (negative omega), the surface low pressure and trough axes, and the midtropospheric trough located just upstream}.

The lack of a spatial association between synoptic features typically promoting upward vertical motion and precipitation in the CCB is evident for certain $\mathbf{V}(500)$ and convection joint classes in the two summers, further suggesting a land surface mesoscale contribution (Part II). For example, on MF/CV days in 2000 (Fig. 9a) the swath of high precipitation amounts in southern areas of Illinois and Indiana has no obvious connection with the synoptic composite anomalies denoting baroclinity (Fig. 8c), which are juxtaposed spatially to the northwest. On MF/CV days in 1999 (Fig. 9b), precipitation in parts of Missouri averaged more than in the Upper Midwest, even though the composite

synoptic conditions (Fig. 7c) do not appear to favor the former location (e.g., upper ridge and dry lower troposphere). Interaction of the low-level, broad southwesterly flow with the Ozark Plateau may have been important for these precipitation higher values. Also not readily explained by the synoptic composites for MF/CV (i.e., in 1999) days, the increased precipitation in central Michigan and eastern Ohio shows midtropospheric ridging and SH(850) negative anomalies over these areas (cf. Figs. 7c and 9b). Spatial incongruities of synoptic circulation–precipitation composite patterns such as these imply the presence of additional climatic factors promoting deep convection; particularly, land surface mesoscale conditions. These are examined in Part II.

6. Summary and concluding remarks

This is Part I of a two-part observational study to determine the relative influences of synoptic atmospheric circulation ("top down") and land surface mesoscale ("bottom up") conditions on convective precipitation for the Midwest CCB in the contrasting summer seasons of 1999 (dry) and 2000 (normal to moist), set within the context of the six-summer period 1996–2001. Our empirical approach contrasts with many studies of land surface–climate interactions, especially for the Great Plains, which emphasize numerical modeling. We determined the stratified composite relationships among NNR tropospheric variables representing the synoptic circulation (e.g., geopotential height, SLP, omega, and winds), radar-indicated deep convective activity for the afternoon and evening hours (i.e., presence/absence and morphological signature type), and once-daily (early morning) station totals of precipitation. For both summers there is strong consistency (i.e., spatial patterns and magnitudes) between atmospheric circulation anomalies and the precipitation when each climate parameter is averaged temporally. Daily frequencies of background wind speed and convective activity differ between the two study summers, and also with respect to the 1996–2001 summer-season means of these indices. In the summer of 1999, radar echoes signifying nonorganized deep convection increased most at the slowest background wind speeds, and organized nonlinear convection type decreased in frequency at the stronger wind speeds. The summer of 2000 mostly saw the opposite pattern.

Despite large between-summer (i.e., 1999 and 2000) differences in convective activity and associated precipitation for the CCB, broad similarities are evident in the synoptic composite anomaly fields for days of deep convection (CV) stratified by background flow strength, as follows: 1) radar-indicated convection on WF and W-MF days was less organized than on J days; 2) precipitation on J days was heaviest and spatially most homogeneous in the divergent region just downstream of the upper-tropospheric u-wind positive anomaly [i.e., $u(300)$]; 3) the day following convection associated with a jet maximum (i.e., J/CV) was classified typically as "jet maximum/no convection" ("J/NC") in the CCB, reflecting the well-known synoptic "cycle" in this region during summer (e.g., Schubert et al. 1998; Bentley and Stallins 2007); and 4) synoptic composite fields for CV and NC days were more similar to each other on weaker flow days than they were on strong flow days.

Schematic maps of tropospheric composite anomaly features compiled for the $\mathbf{V}(500)$ categories separately for the two study summers confirm the following synoptic associations with afternoon and evening radar-indicated convection in the CCB and larger Midwest region: low pressure incoming from the west, southerly low-level wind maximum resembling an LLJ, positive anomalies of specific humidity in the lower troposphere, ascending air in midtroposphere, and a location south or southeast of the upper-tropospheric jet. Conversely on NC composite days, the associations comprise a high pressure center or ridging, lower-tropospheric northerly winds and negative anomalies of specific humidity, sinking air in midtroposphere, and either no upper-tropospheric jet or one located south of the area. From the associations demonstrated between radar-indicated deep convection, surface-recorded precipitation, and synoptic circulation as background wind speeds increase, we conclude that hypothesis 1 essentially is confirmed for the CCB.

The NC composites for some $\mathbf{V}(500)$ categories show wind maxima at 850 hPa reminiscent of northerly LLJs in the Great Plains. Moreover, some summer-averaged high precipitation amounts (e.g., the Upper Midwest in summer 1999) are juxtaposed with multiple features indicating baroclinity; particularly, a southerly LLJ intersecting a moisture axis on the south side of the upper-tropospheric jet. By contrast, other high-precipitation areas—notably, those extending from southern Illinois into Indiana in summer 2000—occurred on weaker flow days for which the associated synoptic composite features do not favor widespread or organized convection. These Part I synoptic composites provide the top-down framework within which the complementary role of land surface mesoscale conditions in convective precipitation for the CCB during the two summers is investigated (Part II).

Acknowledgments. This research was supported by NSF ATM Grants 9876753, 9876823, and 9876828. We are grateful to the following student research assistants: Gordon Strassberg (PSU and Ball State University), Leia Jamieson and Chris Ruelle (UWW), and Angela Burkhardt (Ball State University). The comments of the anonymous reviewers on the first submission of this paper were of great benefit when revising the manuscript, which was undertaken while the first author was the EESI Scholar-in-Residence (January–July 2007).

REFERENCES

Adegoke, J. O., R. A. Pielke Sr., J. Eastman, R. Mahmood, and K. G. Hubbard, 2003: Impact of irrigation on midsummer surface fluxes and temperature under dry synoptic conditions: A regional atmospheric model study of the U.S. High Plains. *Mon. Wea. Rev.,* **131,** 556–564.

——, S. Vezhapparambu, C. L. Castro, R. A. Pielke Sr., and A. M. Carleton, 2006: Influence of variations in low-level moisture and soil moisture on the organization of summer convective systems in the U.S. Midwest. Preprints, *18th Conf. on Climate Variability and Change/20th Conf. on Hydrology,* Atlanta, GA, Amer. Meteor. Soc., J5.12. [Available online at http://ams.confex.com/ams/pdfpapers/104829.pdf.]

——, R. A. Pielke Sr., and A. M. Carleton, 2007: Observational and modeling studies of the impacts of agriculture-related land use change on planetary boundary layer processes in the central U.S. *Agric. For. Meteor.,* **142,** 203–215.

Alfaro, E. J., A. Gershunov, and D. Cayan, 2006: Prediction of summer maximum and minimum temperature over the central and western United States: The role of soil moisture and sea surface temperature. *J. Climate,* **19,** 1407–1421.

Anderson, C. J., and R. W. Arritt, 2001: Representation of summertime low-level jets in the central United States by the NCEP–NCAR reanalysis. *J. Climate,* **14,** 234–247.

Arritt, R. W., T. D. Rink, M. Segal, D. P. Todey, C. A. Clark, M. J. Mitchell, and K. M. Labas, 1997: The Great Plains low-level jet during the warm season of 1993. *Mon. Wea. Rev.,* **125,** 2176–2192.

Ashley, W. S., T. L. Mote, P. G. Dixon, S. L. Trotter, E. J. Powell, J. D. Durkee, and A. J. Grundstein, 2003: Distribution of mesoscale convective complex rainfall in the United States. *Mon. Wea. Rev.,* **131,** 3003–3017.

Baidya Roy, S. B., G. C. Hurtt, C. P. Weaver, and S. W. Pacala, 2003: Impact of historical land cover change on the July climate of the United States. *J. Geophys. Res.,* **108,** 4793, doi:10.1029/2003JD003565.

Banta, R. M., R. K. Newsom, J. K. Lundquist, Y. L. Pichugina, R. L. Coulter, and L. Mahrt, 2002: Nocturnal low-level jet characteristics over Kansas during Cases-99. *Bound.-Layer Meteor.,* **105,** 221–252.

Barnston, A. G., and P. T. Schickedanz, 1984: The effect of irrigation on warm season precipitation in the southern Great Plains. *J. Climate Appl. Meteor.,* **23,** 865–888.

Bentley, M. L., and J. A. Stallins, 2007: Synoptic evolution of Midwestern U.S. extreme dew point events. *Int. J. Climatol.,* in press, doi:10.1002/joc.1626.

Betts, A. K., 2004: Understanding hydrometeorology using global models. *Bull. Amer. Meteor. Soc.,* **85,** 1673–1688.

——, J. H. Hall, A. C. M. Beljaars, M. J. Miller, and P. A. Viterbo, 1996: The land surface-atmosphere interaction: A review based on observational and modeling perspectives. *J. Geophys. Res.,* **101,** 7209–7225.

Birmingham, D. L., and P. J. Lamb, 1994: Diagnostics of growing season rainfall fluctuations in central North America. *Proc. 18th Annual Climate Diagnostics Workshop,* Washington, D.C., U.S. Dept. of Commerce, 283–286.

Bluestein, H. B., 1993: *Observations and Theory of Weather Systems.* Vol. II, *Synoptic-Dynamic Meteorology in Midlatitudes,* Oxford University Press, 594 pp.

——, and P. C. Banacos, 2002: The vertical profile of wind and temperature in cyclones and anticyclones over the eastern two-thirds of the United States: A climatology. *Mon. Wea. Rev.,* **130,** 477–506.

Bonan, G. B., 2001: Observational evidence for reduction of daily maximum temperature by croplands in the Midwest United States. *J. Climate,* **14,** 2430–2442.

Bonner, W. D., 1968: Climatology of the low level jet. *Mon. Wea. Rev.,* **96,** 833–850.

Bosilovich, M. G., and S. D. Schubert, 2001: Precipitation recycling over the central United States diagnosed from the *GEOS-1* data assimilation system. *J. Hydrometeor.,* **2,** 26–35.

Brown, M. E., and D. L. Arnold, 1998: Land surface-atmosphere interactions associated with deep convection in Illinois. *Int. J. Climatol.,* **18,** 1637–1653.

Brown, R. D., B. Brasnett, and D. Robinson, 2003: Gridded North American monthly snow depth and snow water equivalent for GCM evaluation. *Atmos.–Ocean,* **41,** 1–14.

Brubaker, K. L., P. A. Dirmeyer, A. Sudradjet, B. S. Levy, and F. Bernal, 2001: A 36-yr climatological description of the evaporative sources of warm-season precipitation in the Mississippi River basin. *J. Hydrometeor.,* **2,** 537–557.

Burde, G. I., A. Zangvil, and P. J. Lamb, 1996: Estimating the role of local evaporation in precipitation for a two-dimensional region. *J. Climate,* **9,** 1328–1338.

Byerle, L. A., and J. Paegle, 2003: Modulation of the Great Plains low-level jet and moisture transports by orography and large-scale circulations. *J. Geophys. Res.,* **108,** 8611, doi:10.1029/2002JD003005.

Cammas, J.-P., and D. Raymond, 1989: Analysis and diagnosis of the composition of ageostrophic circulations in jet-front systems. *Mon. Wea. Rev.,* **117,** 2447–2462.

Carbone, R. E., J. D. Tuttle, D. A. Ahijevych, and S. B. Trier, 2002: Inferences of predictability associated with warm season precipitation episodes. *J. Atmos. Sci.,* **59,** 2033–2056.

Carleton, A. M., 1999: Methodology in climatology. *Ann. Assoc. Amer. Geogr.,* **89,** 713–735.

——, D. Jelinski, D. Travis, D. Arnold, R. Brinegar, and D. Easterling, 1994: Climatic-scale vegetation-cloud interactions during drought using satellite data. *Int. J. Climatol.,* **14,** 593–623.

——, J. Adegoke, J. Allard, D. L. Arnold, and D. J. Travis, 2001: Summer season land cover—Convective cloud associations for the Midwest U.S. "Corn Belt." *Geophys. Res. Lett.,* **28,** 1679–1682.

——, D. J. Travis, J. O. Adegoke, D. L. Arnold, and S. Curran, 2008: Synoptic circulation and land surface influences on convection in the Midwest U.S. "Corn Belt," summers 1999 and 2000. Part II: Role of vegetation boundaries. *J. Climate,* **21,** 3635–3659.

Carlson, T. N., 1991: *Mid-latitude Weather Systems.* Harper Collins Academic, 507 pp.

Changnon, S. A., 2001: Thunderstorm rainfall in the conterminous United States. *Bull. Amer. Meteor. Soc.,* **82,** 1925–1940.

——, 2002: Impacts of the Midwestern drought forecasts of 2000. *J. Appl. Meteor.,* **41,** 1042–1052.

——, 2004: Changing uses of climate predictions in agriculture: Implications for prediction research, providers, and users. *Wea. Forecasting,* **19,** 606–613.

——, and D. Winstanley, 2000: Long-term variations in seasonal weather conditions important to corn production in Illinois. *Climatic Change,* **47,** 353–372.

——, and S. E. Hollinger, 2003: Problems in estimating impacts of future climate change on Midwestern corn yields. *Climatic Change,* **58,** 109–118.

Chase, T. N., R. A. Pielke Sr., T. G. F. Kittel, J. S. Baron, and T. J. Stohlgren, 1999: Potential impacts on Colorado Rocky Mountain weather due to land use changes on the adjacent Great Plains. *J. Geophys. Res.,* **104,** 16 673–16 690.

Chen, F., and R. Avissar, 1994a: Impact of land-surface moisture variability on local shallow convective cumulus and precipitation in large-scale models. *J. Appl. Meteor.,* **33,** 1382–1401.

——, and ——, 1994b: The impact of land-surface wetness heterogeneity on mesoscale heat fluxes. *J. Appl. Meteor.,* **33,** 1323–1340.

Chen, T.-C., and J. A. Kpaeyeh, 1993: The synoptic-scale environment associated with the low-level jet of the Great Plains. *Mon. Wea. Rev.,* **121,** 416–420.

Cheng, W. Y. Y., and W. R. Cotton, 2004: Sensitivity of a cloud-resolving simulation of the genesis of a mesoscale convective system to horizontal heterogeneities in soil moisture initialization. *J. Hydrometeor.,* **5,** 934–958.

Connor, G. J., and F. Woodcock, 2000: The application of synoptic stratification to precipitation forecasting in the trade wind regime. *Wea. Forecasting,* **15,** 276–297.

Copeland, J. H., R. A. Pielke, and T. G. F. Kittel, 1996: Potential climatic impacts of vegetation change: A regional modeling study. *J. Geophys. Res.,* **101,** 7409–7418.

Coughlan, M., and R. Avissar, 1996: The Global Energy and Water Cycle Experiment (GEWEX) Continental-Scale International Project (GCIP): An overview. *J. Geophys. Res.,* **101,** 7139–7147.

Crook, N. A., 1996: Sensitivity of moist convection forced by boundary layer processes to low-level thermodynamic fields. *Mon. Wea. Rev.,* **124,** 1767–1785.

Dalu, G. A., R. A. Pielke Sr., P. L. Vidale, and M. Baldi, 2000: Heat transport and weakening of atmospheric stability induced by mesoscale flows. *J. Geophys. Res.,* **105** (D7), 9349–9363.

Davis, C. A., and S. B. Trier, 2002: Cloud resolving simulations of mesoscale vortex intensification and its effect on a serial mesoscale convective system. *Mon. Wea. Rev.,* **130,** 2839–2858.

——, and Coauthors, 2004: The Bow Echo and MCV Experiment: Observations and opportunities. *Bull. Amer. Meteor. Soc.,* **85,** 1075–1093.

Dirmeyer, P. A., 2003: The role of the land surface background state in climate predictability. *J. Hydrometeor.,* **4,** 599–610.

——, M. J. Fennessy, and L. Marx, 2003: Low skill in dynamical prediction of boreal summer climate: Grounds for looking beyond sea surface temperature. *J. Climate,* **16,** 995–1002.

Dominguez, F., and P. Kumar, 2005: Dominant modes of moisture flux anomalies over North America. *J. Hydrometeor.,* **6,** 194–209.

Doran, J. C., and S. Zhong, 2000: A study of the effects of subgrid-scale land use differences on atmospheric stability in prestorm environments. *J. Geophys. Res.,* **105** (D7), 9381–9392.

——, and ——, 2002: Comments on "Atmospheric disturbance caused by human modification of the landscape." *Bull. Amer. Meteor. Soc.,* **83,** 277–279.

Doswell, C. A., III, 1987: The distinction between large-scale and mesoscale contribution to severe convection: A case study example. *Wea. Forecasting,* **2,** 3–16.

Douville, H., 2003: Assessing the influence of soil moisture on seasonal climate variability with AGCMs. *J. Hydrometeor.,* **4,** 1044–1066.

Durre, I., J. M. Wallace, and D. P. Lettenmaier, 2000: Dependence of extreme daily maximum temperatures on antecedent soil moisture in the contiguous United States during summer. *J. Climate,* **13,** 2641–2651.

Easterling, D. R., 1989: Regionalization of thunderstorm rainfall in the contiguous U.S. *Int. J. Climatol.,* **9,** 567–579.

Elliott, R. D., 1949: Forecasting the weather. *Weatherwise,* **2,** 15–18, 40–43, 64–67, 86–88, 110–113, 136–138.

Englehart, P. J., and A. V. Douglas, 2002: On some characteristic variations in warm season precipitation over the central United States (1910-2000). *J. Geophys. Res.,* **107,** 4286, doi:10.1029/2001JD000972.

Fennessy, M. J., and J. Shukla, 1999: Impact of initial soil wetness on seasonal atmospheric prediction. *J. Climate,* **12,** 3167–3180.

Findell, K. L., and E. A. B. Eltahir, 2003a: Atmospheric controls on soil moisture–boundary layer interactions. Part I: Framework development. *J. Hydrometeor.,* **4,** 552–569.

——, and ——, 2003b: Atmospheric controls on soil moisture–boundary layer interactions. Part II: Feedbacks within the continental United States. *J. Hydrometeor.,* **4,** 570–583.

Fritsch, J. M., R. J. Kane, and C. R. Chelius, 1986: The contribution of the mesoscale convective weather systems to the warm-season precipitation of the United States. *J. Climate Appl. Meteor.,* **25,** 1333–1345.

Gaffen, D. J., and R. J. Ross, 1999: Climatology and trends of U.S. surface humidity and temperature. *J. Climate,* **12,** 811–828.

Gale, J. J., W. A. Gallus Jr., and K. A. Jungbluth, 2002: Toward improved prediction of mesoscale convective system dissipation. *Wea. Forecasting,* **17,** 856–872.

Giorgi, F., L. O. Mearns, C. Shields, and L. Mayer, 1996: A regional model study of the importance of local versus remote controls of the 1988 drought and the 1993 flood over the central United States. *J. Climate,* **9,** 1150–1162.

Gutowski, W. J., Jr., S. G. Decker, R. A. Donavon, Z. Pan, R. W. Arritt, and E. S. Takle, 2003: Temporal–spatial scales of observed and simulated precipitation in central U.S. climate. *J. Climate,* **16,** 3841–3847.

Hane, C. E., 1986: Extratropical squall lines and rainbands. *Mesoscale Meteorology and Forecasting,* P. S. Ray, Ed., Amer. Meteor. Soc., 359–389.

——, R. M. Rabin, T. M. Crawford, H. B. Bluestein, and M. E. Baldwin, 2002: A case study of severe storm development along a dryline within a synoptically active environment. Part II: Multiple boundaries within a synoptically active environment. *Mon. Wea. Rev.,* **130,** 900–920.

Hanesiak, J. M., R. L. Raddatz, and S. Lobban, 2004: Local initiation of deep convection in the Canadian prairie provinces. *Bound.-Layer Meteor.,* **110,** 455–470.

Haragan, D., 1978: Precipitation climatology for the Texas High Plains. *Tex. J. Sci.,* **30,** 107–123.

Hayes, M. J., and W. L. Decker, 1996: Using NOAA AVHRR data to estimate maize production in the United States Corn Belt. *Int. J. Remote Sens.,* **17,** 3189–3200.

Heim, R. R., J. H. Lawrimore, D. B. Wuertz, A. M. Waple, and T. W. R. Wallis, 2003: The REDTI and MSI: Two new national climate impact indices. *J. Appl. Meteor.,* **42,** 1435–1442.

Hicke, J. A., and D. B. Lobell, 2004: Spatiotemporal patterns of cropland area and net primary production in the central United States estimated from USDA agricultural information. *Geophys. Res. Lett.,* **31,** L20502, doi:10.1029/2004GL020927.

Higgins, R. W., Y. Yao, E. S. Yarosh, J. E. Janowiak, and K. C. Mo, 1997: Influence of the Great Plains low-level jet on summertime precipitation and moisture transport over the central United States. *J. Climate,* **10,** 481–507.

Hong, S.-Y., and E. Kalnay, 2002: The 1998 Oklahoma–Texas drought: Mechanistic experiments with NCEP global and regional models. *J. Climate,* **15,** 945–963.

Houze, R. A., Jr., 2004: Mesoscale convective systems. *Rev. Geophys.,* **42,** RG4003, doi:10.1029/2004RG000150.

Hu, Q., and S. Feng, 2001: Climatic role of the southerly flow from the Gulf of Mexico in interannual variations in summer rainfall in the central United States. *J. Climate,* **14,** 3156–3170.

——, and G. Buyanovsky, 2003: Climate effects on corn yield in Missouri. *J. Appl. Meteor.,* **42,** 1626–1635.

——, and S. Feng, 2003: A daily soil temperature dataset and soil temperature climatology of the contiguous United States. *J. Appl. Meteor.,* **42,** 1139–1156.

Huang, J., and H. M. Van den Dool, 1993: Monthly precipitation–temperature relations and temperature prediction over the United States. *J. Climate,* **6,** 1111–1132.

Jirak, I. L., W. R. Cotton, and R. L. McAnelly, 2003: Satellite and radar survey of mesoscale convective system development. *Mon. Wea. Rev.,* **131,** 2428–2449.

Johns, R. H., and C. A. Doswell III, 1992: Severe local storms forecasting. *Wea. Forecasting,* **7,** 588–612.

Joseph, R., M. Ting, and P. Kumar, 2000: Multiple-scale spatio–temporal variability of precipitation over the coterminous United States. *J. Hydrometeor.,* **1,** 373–392.

Kalnay, E., and Coauthors, 1996: The NCEP/NCAR 40-Year Reanalysis Project. *Bull. Amer. Meteor. Soc.,* **77,** 437–471.

Kanae, S., Y. Hirabayashi, T. Yamada, and T. Oki, 2006: Influence of "realistic" land surface wetness on predictability of seasonal precipitation in boreal summer. *J. Climate,* **19,** 1450–1460.

Kistler, R., and Coauthors, 2001: The NCEP–NCAR 50-Year Reanalysis: Monthly means CD-ROM and documentation. *Bull. Amer. Meteor. Soc.,* **82,** 247–267.

Klink, K., 1995: Surface aggregation and subgrid-scale climate. *Int. J. Climatol.,* **15,** 1219–1240.

Koster, R. D., and M. J. Suarez, 1995: Relative contributions of land and ocean processes to precipitation variability. *J. Geophys. Res.,* **100,** 13 775–13 790.

——, and ——, 2004: Suggestions in the observational record of land–atmosphere feedback operating at seasonal time scales. *J. Hydrometeor.,* **5,** 567–572.

——, ——, R. W. Higgins, and H. M. Van den Dool, 2003: Observational evidence that soil moisture variations affect precipitation. *Geophys. Res. Lett.,* **30,** 1241, doi:10.1029/2002GL016571.

——, and Coauthors, 2004: Realistic initialization of land surface states: Impacts on subseasonal forecast skill. *J. Hydrometeor.,* **5,** 1049–1063.

Kunkel, K. E., and X.-Z. Liang, 2005: GCM simulations of the climate in the central United States. *J. Climate,* **18,** 1016–1031.

——, and Coauthors, 1998: An expanded digital daily database for climatic resources applications in the Midwestern United States. *Bull. Amer. Meteor. Soc.,* **79,** 1357–1366.

Liu, J., R. E. Stewart, and K. K. Szeto, 2004: Moisture transport and other hydrometeorological features associated with the severe 2000/01 drought over the western and central Canadian provinces. *J. Climate,* **17,** 305–319.

Lynn, B. H., W.-K. Tao, and P. J. Wetzel, 1998: A study of landscape-generated deep moist convection. *Mon. Wea. Rev.,* **126,** 928–942.

Maddox, R., 1980: Mesoscale convective complexes. *Bull. Amer. Meteor. Soc.,* **61,** 1374–1387.

——, 1983: Large-scale meteorological conditions associated with midlatitude meso-scale convective complexes. *Mon. Wea. Rev.,* **111,** 1475–1493.

——, L. R. Hoxit, and C. F. Chappell, 1980: A study of tornadic thunderstorm interactions with thermal boundaries. *Mon. Wea. Rev.,* **108,** 322–336.

Mahfouf, J.-F., E. Richard, and P. Mascart, 1987: The influence of soil and vegetation on the development of mesoscale circulations. *J. Climate Appl. Meteor.,* **26,** 1483–1495.

Markowski, G. R., and G. R. North, 2003: Climatic influence of sea surface temperature: Evidence of substantial precipitation correlation and predictability. *J. Hydrometeor.,* **4,** 856–877.

Maurer, E. P., and D. P. Lettenmaier, 2003: Predictability of seasonal runoff in the Mississippi River basin. *J. Geophys. Res.,* **108,** 8607, doi:10.1029/2002JD002555.

McCorcle, M. D., 1988: Simulation of surface moisture effects on the Great Plains low-level jet. *Mon. Wea. Rev.,* **116,** 1705–1720.

McPherson, R. A., D. J. Stensrud, and K. C. Crawford, 2004: The impact of Oklahoma's winter wheat belt on the mesoscale environment. *Mon. Wea. Rev.,* **132,** 405–421.

Mitchell, M. J., R. W. Arritt, and K. Labas, 1995: A climatology of the warm season Great Plains low-level jet using wind profiler observations. *Wea. Forecasting,* **10,** 576–591.

Mo, K. C., 2003: Ensemble canonical correlation prediction of surface temperature over the United States. *J. Climate,* **16,** 1665–1683.

——, J. R. Zimmerman, E. Kalnay, and M. Kanamitsu, 1991: A GCM study of the 1988 United States drought. *Mon. Wea. Rev.,* **119,** 1512–1532.

Moller, A. R., C. A. Doswell III, M. P. Foster, and G. R. Woodall, 1994: The operational recognition of supercell thunderstorm environments and storm structures. *Wea. Forecasting,* **9,** 327–347.

Montroy, D. L., M. B. Richman, and P. J. Lamb, 1998: Observed nonlinearities of monthly teleconnections between tropical Pacific sea surface temperature anomalies and central and eastern North American precipitation. *J. Climate,* **11,** 1812–1835.

Moore, J. T., and G. E. VanKnowe, 1992: The effect of jet-streak curvature on kinematic fields. *Mon. Wea. Rev.,* **120,** 2429–2441.

Moore, N., and S. Rojstaczer, 2001: Irrigation-induced rainfall and the Great Plains. *J. Appl. Meteor.,* **40,** 1297–1309.

Namias, J., 1991: Spring and summer 1988 drought over the contiguous United States—Causes and prediction. *J. Climate,* **4,** 54–65.

National Weather Service, 2001: WSR-88D system specification. Doc. 2810000C, Code Identification 0WY55, WSR-88D ROC, 4 May 2001, WSR-88D Radar Operations Center, Norman, OK, 217 pp.

NCDC, 2003: Data documentation for data set 3200 (DSI-3200), Surface Land Daily Cooperative Summary of the Day. National Climate Data Center, Asheville, NC, 21 pp.

Nykanen, D. K., E. Foufoula-Georgiou, and W. M. Lapenta, 2001: Impact of small-scale rainfall variability on larger-scale spatial organization of land–atmosphere fluxes. *J. Hydrometeor.,* **2,** 105–121.

Oglesby, R. J., S. Marshall, J. O. Roads, and F. R. Robertson, 2001: Diagnosing warm season precipitation over the GCIP region from a GCM and reanalysis. *J. Geophys. Res.,* **106** (D4), 3357–3369.

O'Neal, M., 1996: Interactions between land cover and convective cloud cover over Midwestern North America detected from GOES satellite data. *Int. J. Remote Sens.,* **17,** 1149–1181.

Orville, R. E., and G. R. Huffines, 2001: Cloud-to-ground lightning in the United States: NLDN results in the first decade, 1989–98. *Mon. Wea. Rev.,* **129,** 1179–1193.

Pal, J. S., and E. A. B. Eltahir, 2001: Pathways relating soil moisture conditions to future summer rainfall within a model of the land–atmosphere system. *J. Climate,* **14,** 1227–1242.

Pan, Z., M. Segal, R. Turner, and E. Takle, 1995: Model simulation of impacts of transient surface wetness on summer rainfall in the United States Midwest during drought and flood years. *Mon. Wea. Rev.,* **123,** 1575–1581.

Parker, M. D., 2004: Structure and dynamics of quasi-2D mesoscale convective systems. *J. Atmos. Sci.,* **61,** 545–568.

——, and R. H. Johnson, 2000: Organizational modes of midlatitude mesoscale convective systems. *Mon. Wea. Rev.,* **128,** 3413–3436.

Phillips, J., B. Rajagopalan, M. Cane, and C. Rosenzweig, 1999: The role of ENSO in determining climate and maize yield variability in the U.S. Cornbelt. *Int. J. Climatol.,* **19,** 877–888.

Pielke, R. A., Sr., 2001: Influence of the spatial distribution of vegetation and soils on the prediction of cumulus convective rainfall. *Rev. Geophys.,* **39,** 151–177.

——, and X. Zeng, 1989: Influence on severe storm development of irrigated land. *Natl. Wea. Dig.,* **14,** 16–17.

——, G. E. Liston, J. L. Eastman, L. Lu, and M. Coughenour, 1999: Seasonal weather prediction as an initial value problem. *J. Geophys. Res.,* **104** (D16), 19 463–19 479.

Pitchford, K. L., and J. London, 1962: The low-level jet as related to nocturnal thunderstorms over Midwest United States. *J. Appl. Meteor.,* **1,** 43–47.

Portis, D. H., and P. J. Lamb, 1988: Estimation of large-scale vertical motion over the central United States for summer. *Mon. Wea. Rev.,* **116,** 622–635.

Purdom, J. F. W., 1976: Some uses of high-resolution GOES imagery in the mesoscale forecasting of convection and its behavior. *Mon. Wea. Rev.,* **104,** 1474–1483.

Quan, X., M. Hoerling, J. Whitaker, G. Bates, and T. Xu, 2006: Diagnosing sources of U.S. seasonal forecast skill. *J. Climate,* **19,** 3279–3293.

Rabin, R. M., and D. W. Martin, 1996: Satellite observations of shallow cumulus coverage over the central United States: An exploration of land use impact on cloud cover. *J. Geophys. Res.,* **101,** 7149–7155.

——, S. J. Stadler, P. J. Wetzel, D. J. Stensrud, and M. Gregory, 1990: Observed effects of landscape variability on convective clouds. *Bull. Amer. Meteor. Soc.,* **71,** 272–280.

Richman, M. B., and P. J. Lamb, 1985: Climatic pattern analysis of three- and seven-day summer rainfall in the central United States: some methodological considerations and a regionalization. *J. Climate Appl. Meteor.,* **24,** 1325–1343.

Roads, J., and Coauthors, 2003: GCIP water and energy budget synthesis (WEBS). *J. Geophys. Res.,* **108,** 8609, doi:10.1029/2002JD002583.

——, S.-C. Chen, A. K. Guetter, and K. P. Georgakakos, 1994: Large-scale aspects of the United States hydrologic cycle. *Bull. Amer. Meteor. Soc.,* **75,** 1589–1610.

Rotunno, R., J. B. Klemp, and M. L. Weisman, 1988: A theory for strong, long-lived squall lines. *J. Atmos. Sci.,* **45,** 463–485.

Ruiz-Barradas, A., and S. Nigam, 2005: Warm season rainfall variability over the U.S. Great Plains in observations, NCEP and ERA-40 reanalyses, and NCAR and NASA atmospheric model simulations. *J. Climate,* **18,** 1808–1830.

Santanello, J. A., Jr., M. A. Friedl, and W. P. Kustas, 2005: An empirical investigation of convective planetary boundary layer evolution and its relationship with the land surface. *J. Appl. Meteor.,* **44,** 917–932.

Schaaf, C. B., J. Wurman, and R. M. Banta, 1988: Thunderstorm-producing terrain features. *Bull. Amer. Meteor. Soc.,* **69,** 272–277.

Schubert, S. D., H. M. Helfand, C.-Y. Wu, and W. Min, 1998: Sub-seasonal variation in warm-season moisture transport and precipitation over the central and eastern United States. *J. Climate,* **11,** 2530–2555.

Segal, M., and R. W. Arritt, 1992: Nonclassical mesoscale circulations caused by surface sensible heat-flux gradients. *Bull. Amer. Meteor. Soc.,* **73,** 1593–1604.

——, R. Avissar, M. C. McCumber, and R. A. Pielke, 1988: Evaluation of vegetation effects on the generation and modification of mesoscale circulations. *J. Atmos. Sci.,* **45,** 2268–2292.

——, W. E. Schreiber, G. Kallos, J. R. Garratt, A. Rodi, J. Weaver, and R. A. Pielke, 1989: The impact of crop areas in northeast Colorado on midsummer mesoscale thermal circulations. *Mon. Wea. Rev.,* **117,** 809–825.

——, Z. Pan, and R. W. Arritt, 2002: On the effect of relative timing of diurnal and large-scale forcing on summer extreme rainfall characteristics over the central United States. *Mon. Wea. Rev.,* **130,** 1442–1450.

Seneviratne, S. I., P. Viterbo, D. Lüthi, and C. Schär, 2004: Inferring changes in terrestrial water storage using ERA-40 reanalysis data: The Mississippi River Basin. *J. Climate,* **17,** 2039–2057.

Shafer, C. E., and J. W. Mjedle, 1994: Weather, agricultural production and prices. *Handbook of Agricultural Meteorology,* J. F. Griffiths, Ed., Oxford University Press, 299–308.

Sharratt, B. S., J. Zandlo, and G. Spoden, 2001: Frequency of precipitation across the northern U.S. Corn Belt. *J. Appl. Meteor.,* **40,** 183–191.

Shaw, W. J., and J. C. Doran, 2001: Observations of systematic boundary layer divergence patterns and their relationship to land use and topography. *J. Climate,* **14,** 1753–1764.

Smull, B. F., and J. A. Augustine, 1993: Multiscale analysis of a mature mesoscale convective complex. *Mon. Wea. Rev.,* **121,** 103–132.

Sud, Y. C., D. M. Mocko, K.-M. Lau, and R. Atlas, 2003: Simulating the Midwestern U.S. drought of 1988 with a GCM. *J. Climate,* **16,** 3946–3965.

Sudradjat, A., K. L. Brubaker, and P. A. Dirmeyer, 2003: Interannual variability of surface evaporative moisture sources of warm-season precipitation in the Mississippi River basin. *J. Geophys. Res.,* **108,** 8612, doi:10.1029/2002JD003061.

Teuling, A. J., and P. A. Troch, 2005: Improved understanding of soil moisture variability dynamics. *Geophys. Res. Lett.,* **32,** L05404, doi:10.1029/2004GL021935.

Tian, B., I. M. Held, N.-C. Lau, and B. J. Soden, 2005: Diurnal cycle of summertime deep convection over North America: A satellite perspective. *J. Geophys. Res.,* **110,** D08108, doi:10.1029/2004JD005275.

Trapp, R. J., S. A. Tessendorf, E. S. Godfrey, and H. E. Brooks, 2005: Tornadoes from squall lines and bow echoes. Part I: Climatological distribution. *Wea. Forecasting,* **20,** 23–34.

Travis, D. J., 1997: An investigation of Wisconsin's anthropogenically-generated convergence boundary and possible influences on climate. *Wisc. Geogr.,* **12,** 34–46.

Trenberth, K. E., and C. J. Guillemot, 1996: Physical processes involved in the 1988 drought and 1993 floods in North America. *J. Climate,* **9,** 1288–1298.

Tsvetsinskaya, E. A., L. O. Mearns, and W. E. Easterling, 2001: Investigating the effect of seasonal plant growth and development in three-dimensional atmospheric simulations. Part II: Atmospheric response to crop growth and development. *J. Climate,* **14,** 711–729.

Tuttle, J. D., and C. A. Davis, 2006: Corridors of warm season precipitation in the central United States. *Mon. Wea. Rev.,* **134,** 2297–2317.

Twine, T. E., C. J. Kucharik, and J. A. Foley, 2004: Effects of land cover change on the energy and water balance of the Mississippi River Basin. *J. Hydrometeor.,* **5,** 640–655.

Uccellini, L. W., and D. R. Johnson, 1979: The coupling of upper and lower tropospheric jet streaks and implications for the development of severe convective storms. *Mon. Wea. Rev.,* **107,** 682–703.

Van den Dool, H., J. Huang, and Y. Fan, 2003: Performance and analysis of the constructed analogue method applied to U.S. soil moisture over 1981-2001. *J. Geophys. Res.,* **108,** 8617, doi:10.1029/2002JD003114.

Wallace, J. M., and P. V. Hobbs, 1977: *Atmospheric Science, An Introductory Survey*. Academic Press, 467 pp.

Walters, C. K., 2001: Airflow configurations of warm season southerly low-level wind maxima in the Great Plains. Part II: The synoptic and subsynoptic-scale environment. *Wea. Forecasting,* **16,** 531–551.

——, and J. A. Winkler, 2001: Airflow configurations of warm season southerly low-level wind maxima in the Great Plains. Part I: Spatial and temporal characteristics and relationship to convection. *Wea. Forecasting,* **16,** 513–530.

Wang, J., R. L. Bras, and E. A. B. Eltahir, 2000: The impact of observed deforestation on the mesoscale distribution of rainfall and clouds in Amazonia. *J. Hydrometeor.,* **1,** 267–285.

Wannebo, A., and C. Rosenzweig, 2003: Remote sensing of U.S. cornbelt areas sensitive to the El Niño-Southern Oscillation. *Int. J. Remote Sens.,* **24,** 2055–2067.

Weaver, C. P., 2004a: Coupling between large-scale atmospheric processes and mesoscale land–atmosphere interactions in the U.S. southern Great Plains during summer. Part I: Case studies. *J. Hydrometeor.,* **5,** 1223–1246.

——, 2004b: Coupling between large-scale atmospheric processes and mesoscale land–atmosphere interactions in the U.S. southern Great Plains during summer. Part II: Mean impacts of the mesoscale. *J. Hydrometeor.,* **5,** 1247–1258.

——, and R. Avissar, 2001: Atmospheric disturbances caused by human modification of the landscape. *Bull. Amer. Meteor. Soc.,* **82,** 269–282.

——, and ——, 2002: Reply. *Bull. Amer. Meteor. Soc.,* **83,** 280–283.

Weisman, M. L., 1993: The genesis of severe long-lived bow echoes. *J. Atmos. Sci.,* **50,** 645–670.

——, and J. B. Klemp, 1984: The structure and classification of numerically simulated convective storms in directionally varying wind shears. *Mon. Wea. Rev.,* **112,** 2479–2498.

Westcott, N. E., S. E. Hollinger, and K. E. Kunkel, 2005: Use of real-time multisensor data to assess the relationship of normalized corn yield with monthly rainfall and heat stress across the central United States. *J. Appl. Meteor.,* **44,** 1667–1676.

Wetzel, P. J., 1990: A simple parcel method for prediction of cumulus onset and area-averaged cloud amount over heterogeneous land surfaces. *J. Appl. Meteor.,* **29,** 516–523.

——, S. Argentini, and A. Boone, 1996: Role of land surface in controlling daytime cloud amount: Two case studies in the GCIP-SW area. *J. Geophys. Res.,* **101,** 7359–7370.

Whiteman, C. D., X. Bian, and S. Zhong, 1997: Low-level jet climatology from enhanced rawinsonde observations at a site in the southern Great Plains. *J. Appl. Meteor.,* **36,** 1363–1376.

Wilson, J. W., and W. E. Schreiber, 1986: Initiation of convective storms at radar-observed boundary-layer convergence lines. *Mon. Wea. Rev.,* **114,** 2516–2536.

——, G. B. Foote, N. A. Cooke, J. C. Fankhauser, C. G. Wade, J. D. Tuttle, and C. K. Mueller, 1992: The role of boundary-layer convergence zones and horizontal rolls in the initiation of thunderstorms: A case study. *Mon. Wea. Rev.,* **120,** 1785–1815.

Winkler, J. A., B. R. Skeeter, and P. D. Yamamoto, 1988: Seasonal variations in the diurnal characteristics of heavy hourly precipitation across the United States. *Mon. Wea. Rev.,* **116,** 1641–1658.

Xue, Y., M. J. Fennessy, and P. J. Sellers, 1996: Impact of vegetation properties on U.S. summer weather prediction. *J. Geophys. Res.,* **101** (D3), 7419–7430.

Yan, H., and R. A. Anthes, 1988: The effect of variations in soil moisture on mesoscale circulations. *Mon. Wea. Rev.,* **116,** 192–208.

Yang, F., A. Kumar, and K.-M. Lau, 2004: Potential predictability of U.S. summer climate with "perfect" soil moisture. *J. Hydrometeor.,* **5,** 883–895.

Yu, C.-K., B. J.-D. Jou, and B. F. Smull, 1999: Formative stage of a long-lived mesoscale vortex observed by airborne Doppler radar. *Mon. Wea. Rev.,* **127,** 838–857.

Zaitao, P. K., M. Segal, and R. W. Arritt, 2004: Role of topography in forcing low-level jets in the central United States during the 1993 flood-altered terrain simulations. *Mon. Wea. Rev.,* **132,** 396–403.

Zajac, B. A., and S. A. Rutledge, 2001: Cloud-to-ground lightning activity in the contiguous United States from 1995 to 1999. *Mon. Wea. Rev.,* **129,** 999–1019.

Zangvil, A., D. H. Portis, and P. J. Lamb, 2001: Investigation of the large-scale atmospheric moisture field over the Midwestern United States in relation to summer precipitation. Part I: Relationships between moisture budget components on different timescales. *J. Climate,* **14,** 582–597.

——, ——, and ——, 2004: Investigation of the large-scale atmospheric moisture field over the Midwestern United States in relation to summer precipitation. Part II: Recycling of local evapotranspiration and association with soil moisture and crop yields. *J. Climate,* **17,** 3283–3301.

Zipser, E. J., 1982: Use of a conceptual model of the life cycle of mesoscale convective systems to improve very-short-range forecasts. *Nowcasting,* K. Browning, Ed., Academic Press, 191–204.